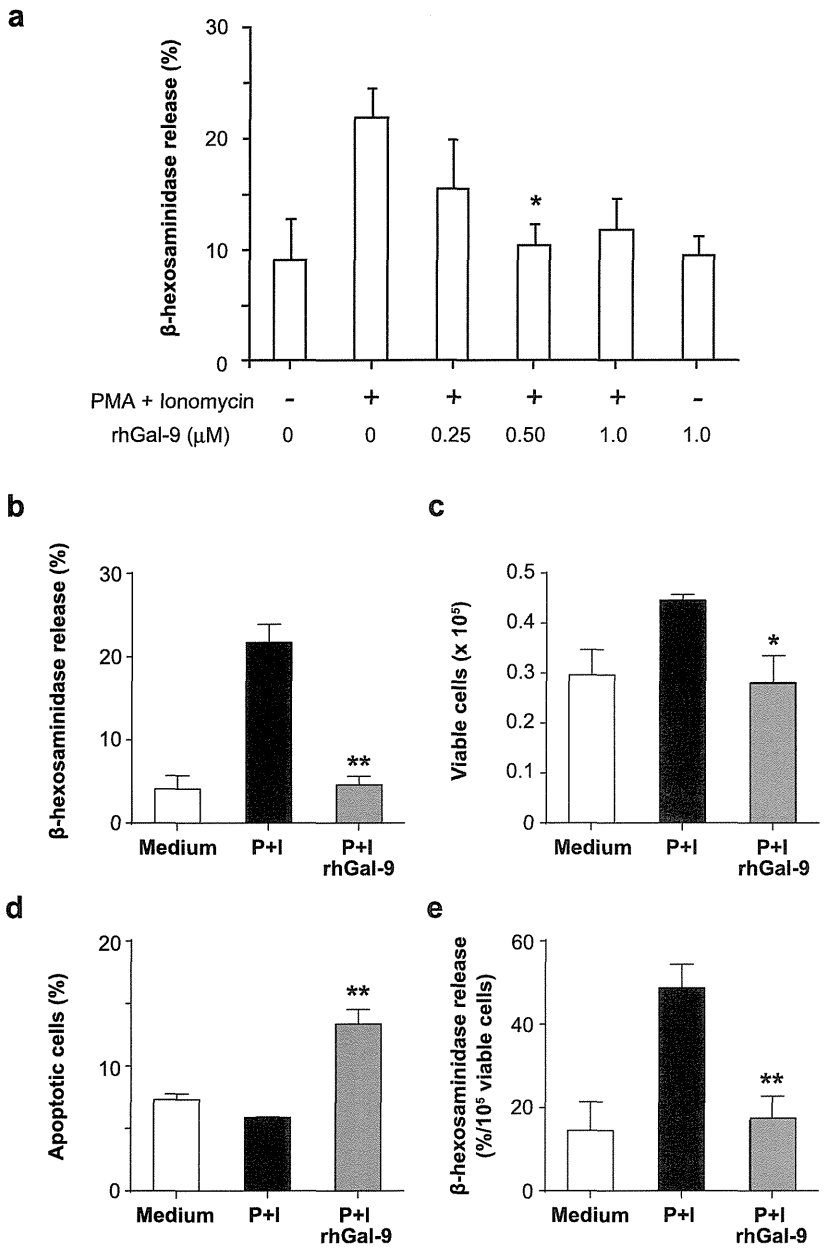

Figure 4. Galectin-9 inhibits PMA- and ionomycin-dependent degranulation of HMC-1 cells. (a, b) HMC-1 cells were treated with 0, 0.25, 0.5 or 1 μM (a) and 0 or 0.5 μM (b) recombinant human galectin-9 (rhGal-9) for 30 min. The cells were then stimulated with 0.1 μg/ml PMA +1 μg/ml ionomycin for 30 min. The level of degranulation was assessed from the activity of β-hexosaminidase in the culture supernatant and plotted as the percent release. (c) The number of viable cells in (b) was determined by trypan blue staining. (d) The proportion of propidium iodide-negative and annexin V-positive apoptotic cells in (b) was assessed by flow cytometry. (e) The relative level of degranulation per live HMC-1 cells was determined as (b)/(c). Data show the mean ± SD of triplicate samples and are a representative result of three (a) or two (b–e) independent experiments. *$p<0.05$, **$p<0.01$ versus PMA+ionomycin alone.
doi:10.1371/journal.pone.0086106.g004

by HMC-1 cells was inhibited by addition of a soluble form of TIM-3 (rhTIM-3/Fc) but not control human IgG (Figure 5c), and by pre-treatment with PD98059 (an ERK1/2 inhibitor) but not SB202474 (control for the ERK1/2 inhibitor) (Figure 5d), suggesting that Gal-9-mediated ERK1/2 activation is required for cytokine production by HMC-1 cells.

Discussion

In the present study, we demonstrated that Gal-9 has dual roles in the functions of a human mast cell line, HMC-1. That is, Gal-9 reduced survival by inducing apoptosis and suppressed degranulation in HMC-1 cells, while it induced cytokine and chemokine production by these cells by activating ERK1/2.

We show that Gal-9 induced phosphorylation of Erk1/2, but not p38 MAPK, in HMC-1 cells (Figure 2). On the other hand, however, Gal-9 induced maturation of human monocyte-derived DCs through activation of p38 MAPK, but not ERK1/2. [34] These observations suggest that the Gal-9-mediated signaling pathway may be different in distinct types of cells. Alternatively, the difference between DCs and HMC-1 cells may be mediated by

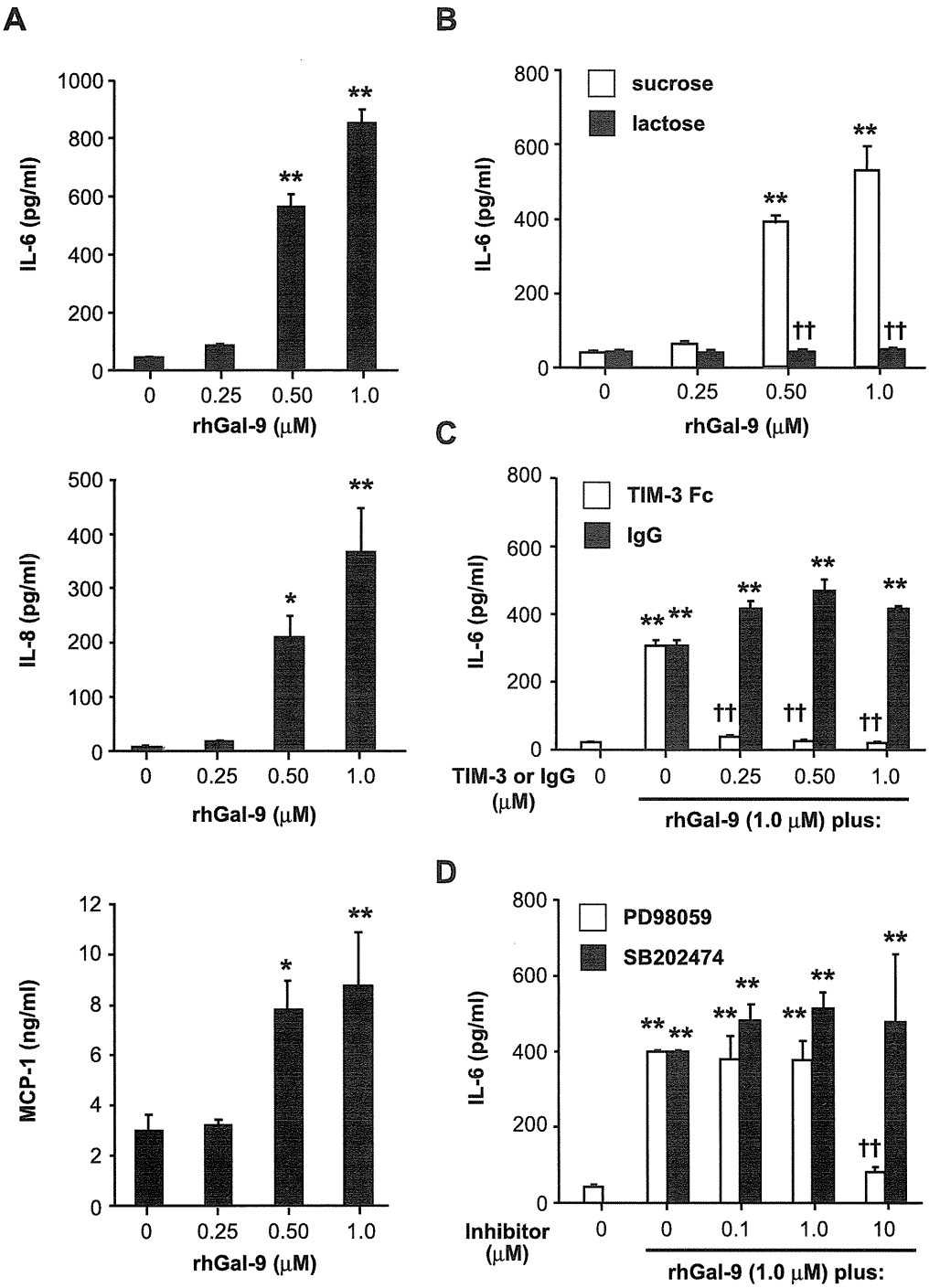

Figure 5. Gal-9 induces cytokine and chemokine production by HMC-1 cells. ELISA was performed to determine the levels of IL-6, IL-8 and MCP-1 in the culture supernatants of HMC-1 cells (**a**), HMC-1 cells pre-treated with 20 mM lactose or sucrose (**b**), HMC-1 cells pre-treated with recombinant human TIM-3/Fc (rhTIM-3/Fc) or control human IgG (human IgG) (**c**) and HMC-1 cells pre-treated with ERK inhibitor (PD98059) or its control (SB202474) (**d**) after 18 hours' stimulation with 0, 0.25, 0.5 or 1 μM recombinant human Galectin-9 (rhGal-9). Data show the mean ± SD of triplicate samples and are a representative result of three independent experiments. *$p<0.05$ and/or **$p<0.01$ versus 0 μM rhGal-9 (**a–d**), and †$p<0.05$ and/or ††$p<0.01$ versus sucrose (**b**), control human IgG (**c**) or ERK inhibitor control (**d**).
doi:10.1371/journal.pone.0086106.g005

distinct receptors such as TIM-3 and unknown molecules that interact with Gal-9. Indeed, the lectin property of Gal-9 was required for Gal-9-mediated cytokine production by HMC-1 cells (Figure 5b), but not by human DCs. [34] In addition, Gal-9 induced apoptosis of HMC-1 cells (Figure 3) as well as thymocytes, Th1 cells and Th17 cells in mice, and human melanoma cell lines. [2,7,21–23,35] In contrast, we previously demonstrated that anti-TIM-3 antibody, which enhanced IgE/Ag-mediated cytokine production as an agonistic antibody, suppressed apoptosis of IL-3-induced mouse bone marrow cell-derived cultured mast cells. [16]

These observations suggest that Gal-9-mediated responses may be dependent or independent of TIM-3, in different cells, since TIM-3 is also known to bind to phosphatidylserine. [36].

It was shown that Gal-9 bound IgE, resulting in inhibition of IgE/antigen-FcεRI-mediated degranulation in mouse mast cell lines by preventing IgE/antigen complex formation. [29] In the present study, because HMC-1 cells do not express FcεRI, [37] we assessed the effect of Gal-9 on PMA/ionomycin-mediated degranulation of HMC-1 cells. Figure 4 shows that Gal-9 suppressed that degranulation both directly and indirectly, suggesting that there might be distinct mechanisms underlying the inhibitory effects of Gal-9 on IgE/antigen-FcεRI-mediated and PMA/ionomycin-mediated mast cell degranulation.

Studies in rodents found that treatment with Gal-9 before antigen challenge resulted in attenuation of ovalbumin- and mite allergen-induced allergic airway inflammation as well as passive cutaneous anaphylaxis after antigen challenge. [27,29] Gal-9's attenuation of such disorders in mast cells [29] was due to suppression of degranulation, rather than induction of cytokines and chemokines, probably independent of TIM-3, since TIM-3-deficient mice normally developed allergic airway inflammation. [28] However, treatment with Gal-9 after antigen challenge may exacerbate inflammation in the late phase of allergic diseases by enhancing cytokine and chemokine production by mast cells and recruiting eosinophils to local inflammatory sites.

In conclusion, Gal-9 appears to play dual roles in the function of human mast cell line. Our results suggest that Gal-9 may modulate the induction and progression of allergic diseases by suppressing degranulation and enhancing cytokine and chemokine production of mast cells. In addition, Gal-9 may be a potential therapeutic target for immediate allergic reactions induced by mast cell degranulation.

Acknowledgments

We are grateful to Lawrence W. Stiver (Tokyo, Japan) for critical reading of the manuscript.

Author Contributions

Conceived and designed the experiments: TO MI S. Nakae. Performed the experiments: RK TO. Analyzed the data: RK TO S. Nakae. Contributed reagents/materials/analysis tools: MI TN MH KI HT S. Nonoyama AM HS KM. Wrote the paper: RK TO S. Nakae.

References

1. Matsumoto R, Hirashima M, Kita H, Gleich GJ (2002) Biological activities of ecalectin: a novel eosinophil-activating factor. J Immunol 168: 1961–1967.
2. Matsumoto R, Matsumoto H, Seki M, Hata M, Asano Y, et al. (1998) Human ecalectin, a variant of human galectin-9, is a novel eosinophil chemoattractant produced by T lymphocytes. J Biol Chem 273: 16976–16984.
3. Matsushita N, Nishi N, Seki M, Matsumoto R, Kuwabara I, et al. (2000) Requirement of divalent galactoside-binding activity of ecalectin/galectin-9 for eosinophil chemoattraction. J Biol Chem 275: 8355–8360.
4. Asakura H, Kashio Y, Nakamura K, Seki M, Dai S, et al. (2002) Selective eosinophil adhesion to fibroblast via IFN-gamma-induced galectin-9. J Immunol 169: 5912–5918.
5. Hirashima M, Kashio Y, Nishi N, Yamauchi A, Imaizumi TA, et al. (2004) Galectin-9 in physiological and pathological conditions. Glycoconj J 19: 593–600.
6. Seki M, Sakata KM, Oomizu S, Arikawa T, Sakata A, et al. (2007) Beneficial effect of galectin 9 on rheumatoid arthritis by induction of apoptosis of synovial fibroblasts. Arthritis Rheum 56: 3968–3976.
7. Wada J, Ota K, Kumar A, Wallner EI, Kanwar YS (1997) Developmental regulation, expression, and apoptotic potential of galectin-9, a beta-galactoside binding lectin. J Clin Invest 99: 2452–2461.
8. Rabinovich GA, Liu FT, Hirashima M, Anderson A (2007) An emerging role for galectins in tuning the immune response: lessons from experimental models of inflammatory disease, autoimmunity and cancer. Scand J Immunol 66: 143–158.
9. Zhu C, Anderson AC, Schubart A, Xiong H, Imitola J, et al. (2005) The Tim-3 ligand galectin-9 negatively regulates T helper type 1 immunity. Nat Immunol 6: 1245–1252.
10. Monney L, Sabatos CA, Gaglia JL, Ryu A, Waldner H, et al. (2002) Th1-specific cell surface protein Tim-3 regulates macrophage activation and severity of an autoimmune disease. Nature 415: 536–541.
11. Nakae S, Iwakura Y, Suto H, Galli SJ (2007) Phenotypic differences between Th1 and Th17 cells and negative regulation of Th1 cell differentiation by IL-17. J Leukoc Biol 81: 1258–1268.
12. Ndhlovu LC, Lopez-Verges S, Barbour JD, Jones RB, Jha AR, et al. (2012) Tim-3 marks human natural killer cell maturation and suppresses cell-mediated cytotoxicity. Blood 119: 3734–3743.
13. Liu Y, Shu Q, Gao L, Hou N, Zhao D, et al. (2010) Increased Tim-3 expression on peripheral lymphocytes from patients with rheumatoid arthritis negatively correlates with disease activity. Clin Immunol 137: 288–295.
14. Tang ZH, Liang S, Potter J, Jiang X, Mao HQ, et al. (2013) Tim-3/galectin-9 regulate the homeostasis of hepatic NKT cells in a murine model of nonalcoholic fatty liver disease. J Immunol 190: 1788–1796.
15. Anderson AC, Anderson DE, Bregoli L, Hastings WD, Kassam N, et al. (2007) Promotion of tissue inflammation by the immune receptor Tim-3 expressed on innate immune cells. Science 318: 1141–1143.
16. Nakae S, Iikura M, Suto H, Akiba H, Umetsu DT, et al. (2007) TIM-1 and TIM-3 enhancement of Th2 cytokine production by mast cells. Blood 110: 2565–2568.
17. Wiener Z, Kohalmi B, Pocza P, Jeager J, Tolgyesi G, et al. (2007) TIM-3 is expressed in melanoma cells and is upregulated in TGF-beta stimulated mast cells. J Invest Dermatol 127: 906–914.
18. Nobumoto A, Oomizu S, Arikawa T, Katoh S, Nagahara K, et al. (2009) Galectin-9 expands unique macrophages exhibiting plasmacytoid dendritic cell-like phenotypes that activate NK cells in tumor-bearing mice. Clin Immunol 130: 322–330.
19. Nagahara K, Arikawa T, Oomizu S, Kontani K, Nobumoto A, et al. (2008) Galectin-9 increases Tim-3+ dendritic cells and CD8+ T cells and enhances antitumor immunity via galectin-9-Tim-3 interactions. J Immunol 181: 7660–7669.
20. Irie A, Yamauchi A, Kontani K, Kihara M, Liu D, et al. (2005) Galectin-9 as a prognostic factor with antimetastatic potential in breast cancer. Clin Cancer Res 11: 2962–2968.
21. Kageshita T, Kashio Y, Yamauchi A, Seki M, Abedin MJ, et al. (2002) Possible role of galectin-9 in cell aggregation and apoptosis of human melanoma cell lines and its clinical significance. Int J Cancer 99: 809–816.
22. Wiersma VR, de Bruyn M, van Ginkel RJ, Sigar E, Hirashima M, et al. (2012) The glycan-binding protein galectin-9 has direct apoptotic activity toward melanoma cells. J Invest Dermatol 132: 2302–2305.
23. Seki M, Oomizu S, Sakata KM, Sakata A, Arikawa T, et al. (2008) Galectin-9 suppresses the generation of Th17, promotes the induction of regulatory T cells, and regulates experimental autoimmune arthritis. Clin Immunol 127: 78–88.
24. Kearley J, McMillan SJ, Lloyd CM (2007) Th2-driven, allergen-induced airway inflammation is reduced after treatment with anti-Tim-3 antibody in vivo. J Exp Med 204: 1289–1294.
25. Sziksz E, Kozma GT, Pallinger E, Komlosi ZI, Adori C, et al. (2010) Galectin-9 in allergic airway inflammation and hyper-responsiveness in mice. Int Arch Allergy Immunol 151: 308–317.
26. Yamamoto H, Kashio Y, Shoji H, Shinonaga R, Yoshimura T, et al. (2007) Involvement of galectin-9 in guinea pig allergic airway inflammation. Int Arch Allergy Immunol 143 Suppl 1: 95–105.
27. Katoh S, Ishii N, Nobumoto A, Takeshita K, Dai SY, et al. (2007) Galectin-9 inhibits CD44-hyaluronan interaction and suppresses a murine model of allergic asthma. Am J Respir Crit Care Med 176: 27–35.
28. Barlow JL, Wong SH, Ballantyne SJ, Jolin HE, McKenzie AN (2011) Tim1 and Tim3 are not essential for experimental allergic asthma. Clin Exp Allergy 41: 1012–1021.
29. Niki T, Tsutsui S, Hirose S, Aradono S, Sugimoto Y, et al. (2009) Galectin-9 is a high affinity IgE-binding lectin with anti-allergic effect by blocking IgE-antigen complex formation. J Biol Chem 284: 32344–32352.
30. Butterfield JH, Weiler D, Dewald G, Gleich GJ (1988) Establishment of an immature mast cell line from a patient with mast cell leukemia. Leuk Res 12: 345–355.
31. Yagami A, Orihara K, Morita H, Futamura K, Hashimoto N, et al. (2010) IL-33 mediates inflammatory responses in human lung tissue cells. J Immunol 185: 5743–5750.
32. Ho LH, Ohno T, Oboki K, Kajiwara N, Suto H, et al. (2007) IL-33 induces IL-13 production by mouse mast cells independently of IgE-FcepsilonRI signals. J Leukoc Biol 82: 1481–1490.
33. Iikura M, Suto H, Kajiwara N, Oboki K, Ohno T, et al. (2007) IL-33 can promote survival, adhesion and cytokine production in human mast cells. Lab Invest 87: 971–978.

34. Dai SY, Nakagawa R, Itoh A, Murakami H, Kashio Y, et al. (2005) Galectin-9 induces maturation of human monocyte-derived dendritic cells. J Immunol 175: 2974–2981.
35. Kashio Y, Nakamura K, Abedin MJ, Seki M, Nishi N, et al. (2003) Galectin-9 induces apoptosis through the calcium-calpain-caspase-1 pathway. J Immunol 170: 3631–3636.
36. Nakayama M, Akiba H, Takeda K, Kojima Y, Hashiguchi M, et al. (2009) Tim-3 mediates phagocytosis of apoptotic cells and cross-presentation. Blood 113: 3821–3830.
37. Xia HZ, Kepley CL, Sakai K, Chelliah J, Irani AM, et al. (1995) Quantitation of tryptase, chymase, Fc epsilon RI alpha, and Fc epsilon RI gamma mRNAs in human mast cells and basophils by competitive reverse transcription-polymerase chain reaction. J Immunol 154: 5472–5480.

Cancer Science
The official journal of the Japanese Cancer Association

Artemis-dependent DNA double-strand break formation at stalled replication forks

Junya Unno,[1,2] Masatoshi Takagi,[1,8] Jinhua Piao,[1] Masataka Sugimoto,[3] Fumiko Honda,[1] Daisuke Maeda,[4,5] Mitsuko Masutani,[4,5] Tohru Kiyono,[6] Fumiaki Watanabe,[1] Tomohiro Morio,[1] Hirobumi Teraoka[7] and Shuki Mizutani[1,8]

[1]Department of Pediatrics and Developmental Biology, Graduate School of Medicine, Tokyo Medical and Dental University, Tokyo; [2]Laboratory of DNA damage signaling, Department of Late Effect Studies, Radiation Biology Center, Kyoto University, Kyoto; [3]Section of Biochemistry, Department of Mechanism of Aging, National Institute for Longevity Sciences, National Center for Geriatrics and Gerontology, Aichi; [4]Biochemistry Division; [5]ADP-ribosylation in Oncology Project; [6]Virology Division, National Cancer Center Research Institute, Tokyo; [7]Department of Pathological Biochemistry, Medical Research Institute, Tokyo Medical and Dental University, Tokyo, Japan

(Received January 22, 2013/Revised February 26, 2013/Accepted March 2, 2013/Accepted manuscript online March 6, 2013/Article first published online April 15, 2013)

Stalled replication forks undergo DNA double-strand breaks (DSBs) under certain conditions. However, the precise mechanism underlying DSB induction and the cellular response to persistent replication fork stalling are not fully understood. Here we show that, in response to hydroxyurea exposure, DSBs are generated in an Artemis nuclease-dependent manner following prolonged stalling with subsequent activation of the ataxia–telangiectasia mutated (ATM) signaling pathway. The kinase activity of the catalytic subunit of the DNA-dependent protein kinase, a prerequisite for stimulation of the endonuclease activity of Artemis, is also required for DSB generation and subsequent ATM activation. Our findings indicate a novel function of Artemis as a molecular switch that converts stalled replication forks harboring single-stranded gap DNA lesions into DSBs, thereby activating the ATM signaling pathway following prolonged replication fork stalling. (*Cancer Sci* 2013; 104: 703–710)

DNA replication is a crucial phase in cell proliferation and is always accompanied by the possibility of generating DNA irregularities. To prevent the disruption of genome integrity during replication by exogenous or endogenous stresses, replication fork progression is precisely regulated and monitored by the replication checkpoint.[1] This machinery is one of the targets for cancer chemotherapy such as alkylating agents or inhibitors of ribonucleotide reductase, which cause an imbalance in the deoxynucleotide triphosphate pool. Stalled replication forks lead to the production of ssDNA lesions including ssDNA gaps, which in some cases are converted to DSBs, an event termed replication fork collapse, by a mechanism in which some nucleases play a key role. Double-strand breaks (DSB) thus generated must be monitored and resolved by DNA damage response mechanisms to maintain genome integrity.

Ataxia–telangiectasia mutated (ATM) is mainly activated by DSBs and recruited to damage sites by the Mre11-Rad50-NBS1 complex.[2] Ataxia-telangiectasia mutated (ATM) exists as an inactive dimer and undergoes autophosphorylation, which triggers monomerization and activation.[3] Another damage-response protein, the ATR–ATR-interacting protein complex, is principally activated by RPA-coated ssDNA regions thatarise at stalled replication forks or during the processing of bulky lesions such as UV photoproducts and DSBs in S/G_2 phases.[4] Once ATM and ATR are activated by DNA lesions, they cooperatively stimulate DNA damage checkpoint pathways through the phosphorylation of numerous substrates, leading to cell cycle arrest, apoptosis, DNA repair, or cell senescence.[5]

The Artemis nuclease is mutated in individuals with RS-SCID. *In vitro*, in the presence of ATP and DNA-PK composed of DNA-PKcs (officially known as protein kinase, DNA-activated, catalytic polypeptide [PRKDC]) and the Ku70/80 heterodimer, Artemis acquires DNA endonuclease activity that specifically targets ssDNA–dsDNA junctions including 5′- or 3′- overhangs, hairpins, and gaps.[6,7] Autophosphorylation of DNA-PKcs at the ABCDE cluster (Thr2609, Ser2612, Thr2620, Ser2624, Thr2638, and Thr2647) is essential for Artemis endonuclease activity.[6] Through its endonuclease activity, Artemis contributes to the repair of a fraction of DSBs (~10%) induced by ionizing radiation *in vivo*, suggesting that it processes the ends of DSBs that are refractory to repair by core non-homologous end joining factors such as Ku70, Ku80, XRCC4, and DNA ligase IV.[8]

Here, we show that the ATR signaling pathway is activated at an early phase of replication fork stalling, and that extensive activation of the ATM signaling pathway is triggered by the generation of DSBs by Artemis nuclease following prolonged replication fork stalling. DNA-PKcs kinase activity is also required for this DSB generation and subsequent ATM activation. Artemis-deficient fibroblasts show resistance to HU. From these results, we propose that the Artemis/DNA-PK machinery plays an essential role in the mechanism that responds to prolonged replication fork stalling by HU.

Materials and Methods

Cells. HeLa, U2OS, M059J, and M059K were obtained from ATCC (Manassas, VA, USA). Human telomerase reverse transcriptase immortalized human diploid fibroblasts (HDF2/326) were described previously. [9]

Immunoblotting and immunofluorescence. Immunoblotting and immunofluorescence were carried out using standard methods. Details of the experimental procedure are also provided in Document S1.

Results

Activation of DNA damage response by HU. To obtain insights into the mechanism by which stalled DNA replication forks are converted to DSBs under certain conditions, we measured the phosphorylation of various ATM/ATR substrates to monitor the status of DNA damage checkpoint activation in response to HU. To assess the effect of HU treatment only in S phase, we synchronized HeLa cells at the G_1-S boundary with a double thymidine block, then released them into S phase for 1 h prior to HU exposure (Fig. S1a). As shown in Figure 1(a), Chk1 Ser345 and NBS1 Ser343 were strongly

[8]To whom correspondence should be addressed.
E-mails: m.takagi.ped@tmd.ac.jp or smizutani.ped@tmd.ac.jp

doi: 10.1111/cas.12144

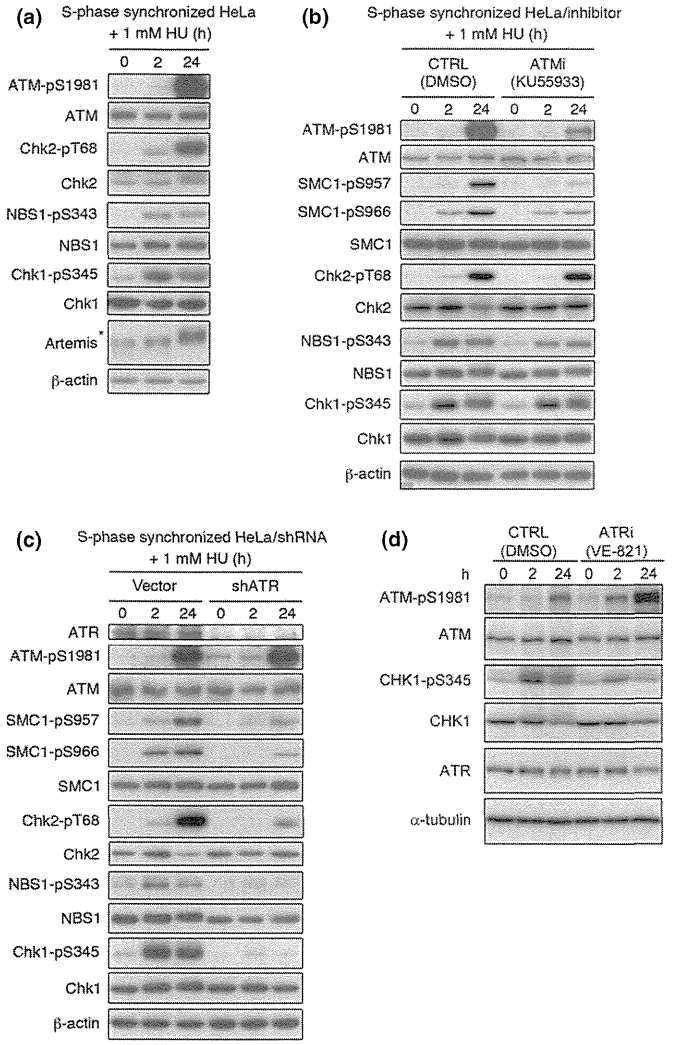

Fig. 1. Ataxia–telangiectasia and RAD3-related (ATR) and ataxia–telangiectasia mutated (ATM) pathways are differentially activated by exposure to hydroxyurea (HU). (a) S-phase synchronized HeLa cells were treated with 1 mM HU 1 h after release from double thymidine block. Cell extracts from the indicated time points were immunoblotted with the indicated antibodies. *Hypersphosphorylated form of Artemis. (b) Synchronized HeLa cells were treated with 1 mM HU 1 h after release from double thymidine blockwith or without ATM-specific inhibitor KU55933 (10 μM). (c) HeLa cells were transfected with shATR-expressing construct or mock vector. The cells were synchronized 24 h after transfection. One hour after release from double thymidine block, cells were treated with 1 mM HU for 2 or 24 h. (d) Synchronized HeLa cells were treated with 1 mM HU 1 h after release from double thymidine blockwith or without ATR-specific inhibitor VE-821 (10 μM). CTRL, control.

phosphorylated after a 2-h exposure to HU. Phosphorylation of ATM at Ser1981 was weakly detectable at 2 h and significantly enhanced after 24 h continuous exposure to HU. Chk2 Thr68 was phosphorylated in parallel with ATM phosphorylation. The activation of the ATM signaling pathway after HU was confirmed by addition of the ATM specific inhibitor KU55933 that attenuated ATM phosphorylation at Ser1981 and SMC1 phosphorylation at Ser957 and Ser966 after HU exposure (Fig. 1b). In contrast, phosphorylation of Chk2, NBS1, and Chk1 was not inhibited by treatment with KU55933 (Fig. 1b, Fig. S1b). As Chk2 was phosphorylated even in ATM-inhibited cells, Chk2 might be phosphorylated by ATR or DNA-PKcs. This result indicates that ATM phosphorylation after HU exposure for 24 h is the result of autophosphorylation, and that ATM preferentially phosphorylates SMC1 after HU exposure.

Previously, phosphorylation of ATM after replication fork stalling has been reported to be dependent on ATR activation.[10] Hence, we investigated whether DNA damage signaling caused by prolonged HU exposure was ATR-dependent using ATR knockdown cells produced with an ATR-specific shRNA[11] (Fig. 1c) or siRNA to target a distinct ATR sequence (Fig. S1c). Increased ATM autophosphorylation was observed after ATR knockdown even in the absence of HU, presumably due to an increase in DSBs or genomic instability caused by ATR depletion.[12] After 2 h exposure to HU, a slightly elevated level of ATM phosphorylation was observed in both cells. After 24 h exposure to HU, ATM was strongly autophosphorylated even in ATR knockdown cells. The ATR knockdown strikingly reduced Chk1 and NBS1 phosphorylation, and partly attenuated Chk2 and SMC1 phosphorylation after both 2 h and 24 h exposure to HU. Although NBS1, Chk2, and SMC1 are well-known ATM targets, NBS1, Chk2, and SMC1 were also phosphorylated in an ATR-dependent manner after HU treatment (Fig. 1c, Fig. S1d). Treatment with the ATR inhibitor VE-821 also represented the siRNA-dependent ATR knockdown experiment (Fig. 1d). These data are consistent with previous reports showing that Chk1, NBS1, and SMC1 are phosphorylated in an ATR-dependent manner after HU or UV exposure[13,14] and that Chk2 can be phosphorylated by ATR *in vitro*.[15] From these results, we concluded that ATM is activated in an ATR-independent manner after prolonged exposure to HU.

Long continuous HU exposure induces DSB. To investigate the precise mechanisms underlying the activation of the ATM signaling pathway after prolonged HU exposure, the concomitant formation of foci of γH2AX, which is indicative of stalled replication forks and DNA DSBs,[16,17] and RPA2, a hallmark of ssDNA lesions, was investigated by immunofluorescence microscopy. γH2AX and RPA2 foci were detectable after a 2-h exposure to HU, although these signals were relatively smaller and weaker than those observed after 24 h exposure. At the 2 h time point, most γH2AX foci colocalized with RPA2 foci (Fig. 2a,b,Fig. S2a). After 24 h HU treatment, γH2AX and RPA2 foci were more intense and granular. Interestingly, although both foci were detectable, most γH2AX foci no longer colocalized with RPA2 foci at this time point (Fig. 2a,b, Fig. S2a,b). After HU treatment, pS1981 phosphorylated ATM formed foci colocalizing with γH2AX in HeLa cells (Fig. S3a). After HU treatment for 24 h, pS1981 phosphorylated ATM was detected as clearly larger foci, and some of these were independent from RPA2 foci in wild-type derived control fibroblasts (WT fibroblasts). However, ATM-pS1981 foci, consisting of weakly stained fine granules, colocalized with RPA2 foci in Artemis-mutated RS-SCID derived AV2/326 cells (Artemis-deficient fibroblasts) (Fig. S3b). These results are compatible with the interpretation that short-term HU exposure causes replication fork arrest and prolonged HU exposure induces DSB, consistent with a previous report indicating the existence of DSB after prolonged HU treatment.[18] To detect DSBs directly, DNA fragmentations after HU exposure were investigated by PFGE. After more than 12 h of HU exposure, increasing amounts of DSBs were clearly generated (Fig. 2c,d). Collectively, observations from Figures 1 and 2 support a two-step model for the activation of DNA damage checkpoints in response to HU-induced replication fork stalling: the primary activation of the ATR signaling as an early phase response to stalled replication fork and the secondary activation of the ATM signaling pathway as a late response to DSB.

Artemis-dependent DSBs activate ATM signaling. Because the relationship between prolonged replication fork stalling and DSB generation has not been precisely clarified, we sought to determine the key factor for DSB formation under these

doi: 10.1111/cas.12144

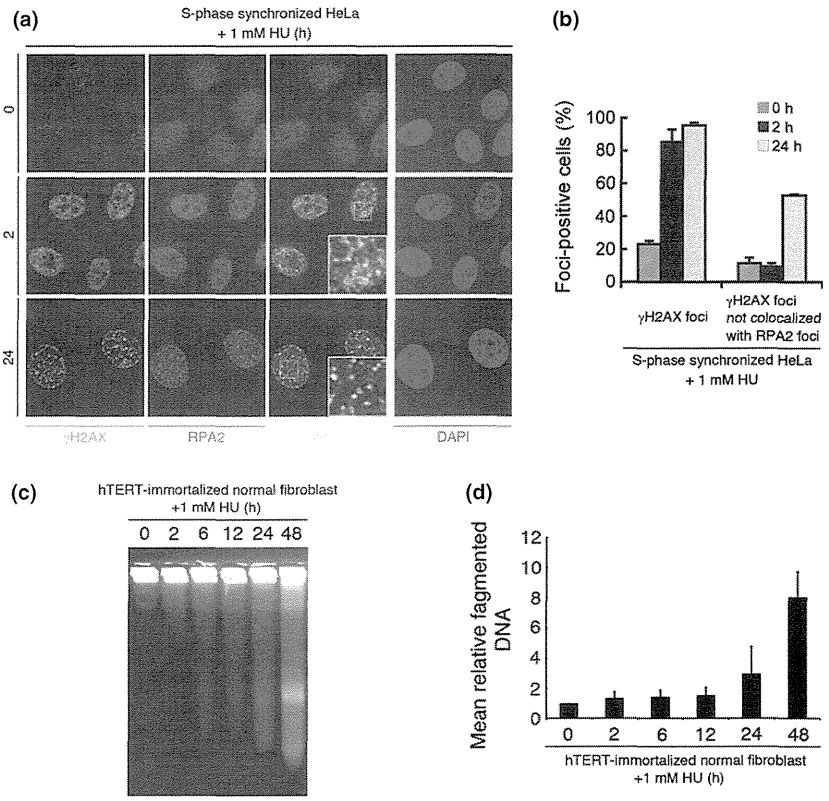

Fig. 2. Short-term hydroxyurea (HU) exposure causes replication fork arrest and 24 h continuous HU exposure induces double-strand breaks (DSB). (a) HeLa cells were synchronized at S phase and treated with 1 mM HU for 2 h or 24 h. Cells were fixed and stained with anti-phosphorylated histone H2AX (γH2AX) (Ser139) and anti-replication protein A2(RPA2) antibodies. (b) More than 100 cells were counted, and the percentage showing >10 γH2AX foci or >4 γH2AX foci not colocalized with RPA2 foci was determined. Data represent the mean ± SEM from three independent experiments. (c) Human telomerase reverse transcriptase (hTERT)-immortalized normal human fibroblasts (HDF2/326) were treated with 1 mM HU for indicated times. Cells were analyzed by pulse field gel electrophoresis (PFGE). (d) Mean relative fragmented DNA (1 = the fraction of DNA released from the gel plug in untreated fibroblasts) from (c) was calculated, and data are shown in the bar graph. Data represent the mean ± SEM from two independent experiments.

conditions. The recruitment of endonuclease(s) to the ssDNA–dsDNA junction, a structure that arises in replication fork stalling, is likely to lead to the generation of DSBs.[16,19] Since the Artemis nuclease is known to process ssDNA–dsDNA junctions *in vitro*,[6,7] we hypothesized that processing of stalled replication forks by the Artemis nuclease leads to generation of DSBs after prolonged HU exposure. To test this possibility, we investigated HU-induced DSBs using WT and Artemis-deficient hTERT-immortalized fibroblasts derived from RS-SCID patients. Pulse field gel electrophoresis (PFGE) showed a lower level of dose-dependent generation of DSBs in Artemis-deficient fibroblasts compared to WT fibroblasts after HU exposure (Fig. 3). Camptothecin treatment was used as a positive control for replication-associated DSB,[11,20] showing no significant difference of DSBs in cells with or without Artemis (Fig. S4a, b). Identical results were obtained with the neutral comet assay, which detects DSBs at the single-cell level, confirming our PFGE data (Fig. S4c,d). These data suggest that DSB generation after prolonged HU exposure is Artemis-dependent.

We also investigated whether the extent of DSB formation induced by HU exposure correlates with the level of DNA damage checkpoint activation. Interestingly, Artemis-deficient fibroblasts treated with HU for 24 h showed attenuated activation of ATM signaling compared to WT fibroblasts (Fig. 4a). To consolidate this finding, we also investigated the effect of Artemis knockdown in HeLa cells using two independent shRNA constructs. These transfectants showed cell cycle kinetics similar to control shRNA-transfected cells (Fig. S5). Artemis knockdown HeLa cells thus generated showed attenuated activation of the ATM signaling pathway after 24 h HU exposure; in contrast, Chk1 phosphorylation levels were unchanged (Fig. 4b). RPA2 was hyperphosphorylated after only 24 h of treatment with 1 mM HU in Artemis-competent cells, as previously described.[11] Interestingly, hyperphosphorylation of RPA2 was attenuated in Artemis-deficient fibroblasts. After DNA damage, ATM, ATR, and DNA-PK dependent phosphorylation of RPA2 plays a key role in replication checkpoint activation. It has been reported hyperphosphorylated RPA2 associates with ssDNA and recombinase protein Rad51 in response to replication arrest by HU treatment and is critical for Rad51 recruitment and homologous recombination-mediated repair.[21] Artemis-deficient cells may also show homologous recombination-mediated DNA repair defect (Fig 4c,d).

To address the functional importance of Artemis nuclease activity, we introduced WT or nuclease dead construct (H254A; histidine to alanine substitution on amino acid 254) of Artemis into Artemis-deficient fibroblasts. As is shown in Figure 4(e), the Artemis nuclease-dead mutant did not promote efficient activation of ATM signaling after HU treatment. This was in contrast to WT transfectant which efficiently restored ATM activation. Chk1 phosphorylation was indistinguishable between the cells expressing WT and nuclease-dead mutant Artemis. These results are in accord with the interpretation that the nuclease activity of Artemis plays a critical role in the generation of DSBs when replication fork stalling is prolonged by long exposure to HU, and that DSBs, thus generated, lead to activation of the ATM-dependent DNA damage response pathway.

DNA-dependent protein kinase (DNA-PK) is activated by replication fork stalling. *In vitro*, Artemis endonuclease activity is controlled by DNA-PKcs autophosphorylation at the ABCDE cluster.[6] Thus, we investigated whether the kinase activity of DNA-PKcs is involved in Artemis-dependent DSB formation and subsequent ATM activation following prolonged HU exposure. To gain direct evidence for the activation of DNA-PKcs, we monitored its autophosphorylation at Ser2056 and/or Thr2609, which have been reported to be essential for DNA-PKcs function.[22,23] A low level of DNA-PKcs Ser2056 phosphorylation was detected after 2 h of HU exposure, which increased after 24 h HU exposure (Fig. 5a, Fig. S6a). Immunofluorescence examination using a phospho-specific antibody against Thr2609 of DNA-PKcs showed similar results in S-phase synchronized HeLa cells, in which we observed small

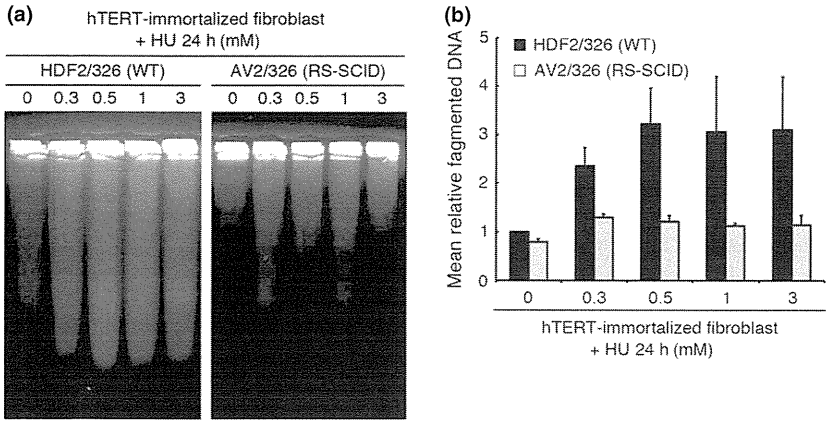

Fig. 3. Double-strand breaks (DSB) generation after replication fork stalling is Artemis-dependent. (a) Human telomerase reverse transcriptase (hTERT)-immortalized normal (HDF2/326;WT) and Artemis-deficient (AV2/326; radiosensitive severe combined immunodeficiency [RS-SCID]) human fibroblasts were treated with the indicated doses of hydroxyurea (HU) for 24 h. Cells were analyzed by pulse field gel electrophoresis (PFGE). (b) Mean relative fragmented DNA (1 = the fraction of DNA released from the gel plug in untreated fibroblasts) from (a) was calculated, and data are shown in the bar graph. Data represent the mean ± SEM from two independent experiments.

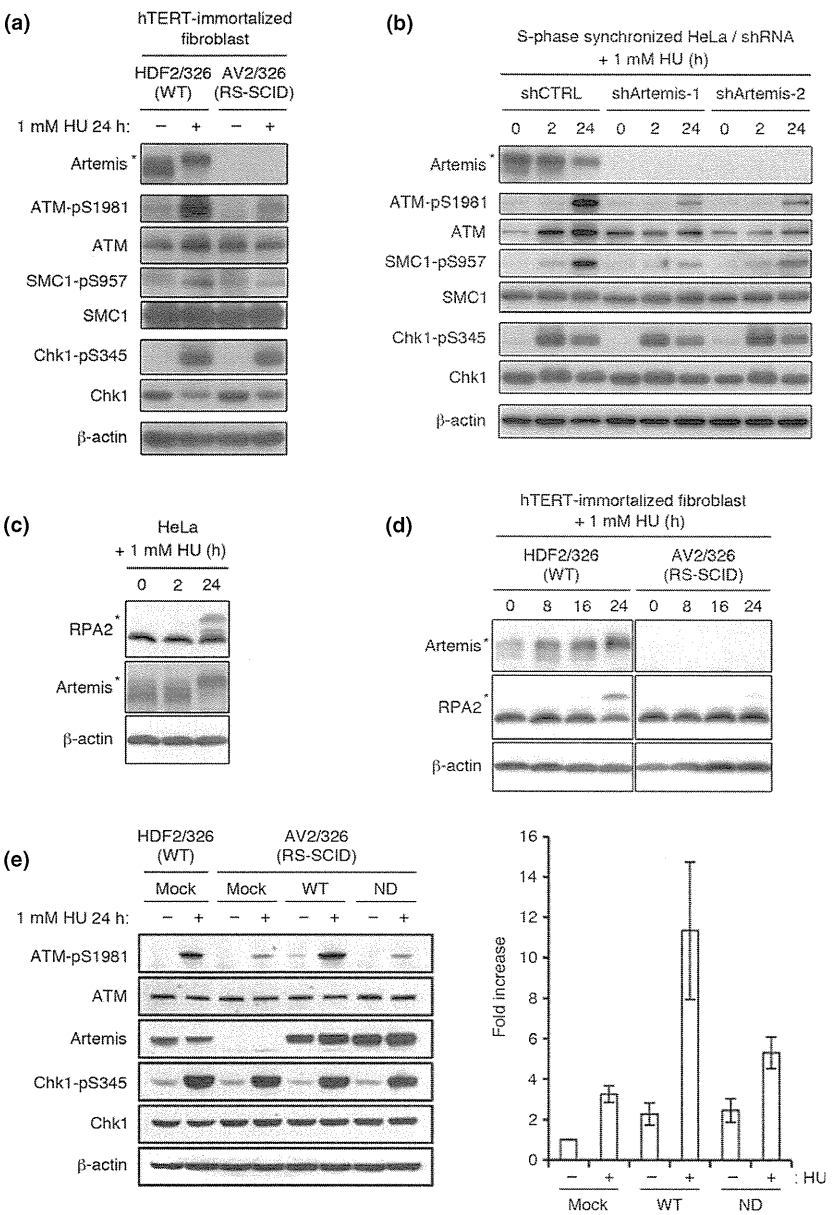

Fig. 4. Activation of the ataxia–telangiectasia mutated (ATM) signaling pathway is Artemis-dependent. (a) HDF2/326 and AV2/326 (radiosensitive severe combined immunodeficiency [RS-SCID] human fibroblasts were treated with 1 mM hydroxyurea (HU) for 24 h. Cell extracts were immunoblotted with the indicated antibodies. (b) HeLa cells were transfected with a control (shCTRL) or two types of shArtemis-expressing construct. Cells were synchronized 24 h after transfection. One hour after release, the cells were treated with 1 mM HU for 2 h or 24 h, and cell extracts were immunoblotted. (c) HeLa cells were treated with 1 mU HU and RPA2 phosphorylation status was determined by Western blotting. (d) Western blot analysis of RPA2 phosphorylation status in HDF2/326 and AV2/326 human fibroblasts. (e) HDF2/326 and AV2/326 human fibroblasts were infected with mock or Artemis WT or H254A nuclease dead mutant (ND). Cells were treated with 1 mM HU for 24 h and subjected to Western blot analysis. Right graph indicates relative ATM phosphorylation standardized to 1 as the base level of mock transduced Artemis-deficient fibroblasts before HU treatment. Data represent the mean ± SEM from three independent experiments. hTERT, human telomerase reverse transcriptase. *Hypersphosphorylated form of Artemis or RPA2.

foci of phospho-DNA-PKcs after a 2 h HU exposure and an increased number and intensity of foci after 24 h HU exposure. These phospho-DNA-PKcs foci colocalized with RPA2 foci following 2 h exposure to HU and remained colocalized even after 24 h exposure (Fig. 5b, Fig. S6b), indicating that DNA-PKcs is activated on stalled replication forks.

Because DNA-PK has been shown to bind to dsDNA ends and is believed to require dsDNA ends for its activation,[24,25]

doi: 10.1111/cas.12144

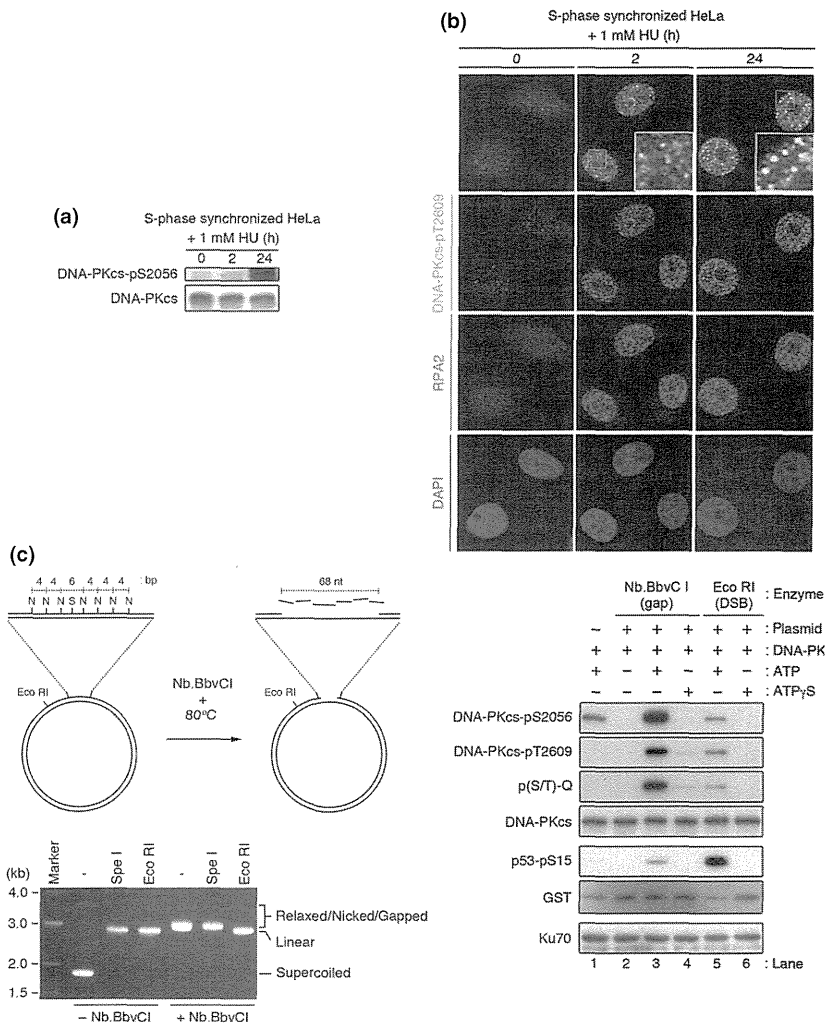

Fig. 5. Activation of catalytic subunit of DNA-dependent protein kinase (DNA-PKcs) by stalled replication forks after treatment with hydroxyurea (HU). (a) S-phase synchronized HeLa cells were treated with 1 mM HU 1 h after release from double thymidine block. Cell extracts from the indicated time points were immunoblotted with an anti-phospho-DNA-PKcs (Ser2056) and generic DNA-PKcs antibody. (b) Same as in (a), cells were stained with anti-phospho-DNA-PKcs (Thr2609) and anti-RPA2 antibodies. (c) Left panel, generation of a single-stranded gap region on pG68 plasmid. Nb.BbvCI digestion generated a nick on the plasmid, and subsequent heat denaturation released DNA fragments. N, Nb.BbvCI site; S, SpeI site. Lower panel, restriction digestion analysis with indicated enzymes. Nb.BbvCI-treated pG68 plasmid was resistant to SpeI digestion (different mobility from EcoRI digestion), indicating the existence of a single-stranded DNA gap in the plasmid. The DNA-PK holoenzyme is activated by a plasmid containing a single-stranded gap DNA *in vitro*. The reaction was analyzed, followed by SDS-PAGE and immunoblotting using indicated antibodies.

our results in Figure 5(a,b) are difficult to interpret. However, several reports have suggested that DNA-PKcs exerts kinase activity at ssDNA–dsDNA junctions in the absence of a dsDNA end *in vitro*.[25,26] The Ku heterodimer is also able to bind to ssDNA–dsDNA junctions *in vitro*.[27] Therefore, we monitored autophosphorylation of DNA-PKcs (Ser2056, Thr2609, and phospho-(S/T)Q) and phosphorylation of p53 peptide (amino acids 1–100) as an indicator of kinase activity to investigate whether ssDNA gaps could activate DNA-PK. To activate DNA-PK, we used a pG68 plasmid carrying an array of seven Nb.BbvCI and one Eco RI sites.[28] Nb.BbvCI or EcoRI treatment created a single-stranded gap DNA region or dsDNA ends on the plasmid, respectively (Fig. 5c). These enzyme-treated plasmids facilitated autophosphorylation of DNA-PKcs only in the presence of ATP (Fig. 5c, lanes 3,5), as assays performed without ATP or with non-hydrolysable ATPγS were unable to support DNA-PKcs autophosphorylation (Fig. 5c, lanes 2,4,6). p53 peptide was preferentially phosphorylated in the presence of dsDNA end than single-stranded gap DNA, which is in accordance with the results of previous studies that used oligonucleotide as activating DNA.[25–27] Thus, our *in vitro* findings strongly support the interpretation that HU-induced stalled replication forks activate DNA-PKcs *in cellulo*. Therefore, we can conclude that DNA-PKcs is activated on stalled replication forks (which are presumably single-stranded gap DNA lesions harboring ssDNA–dsDNA junctions) by HU exposure.

Next, we addressed the relationship between activation of DNA-PKcs and Artemis *in cellulo*. Autophosphorylation of DNA-PKcs was detected in WT and Artemis-deficient fibroblasts following exposure to HU (Fig. S6c). Immunofluorescence microscopy revealed that autophosphorylated DNA-PKcs (Thr2609) foci were also formed in the absence of Artemis after HU exposure, with an almost equal percentage of foci-positive cells in WT and Artemis-deficient fibroblasts (Fig. S6d). These results suggest that the activation of DNA-PKcs by HU treatment is not Artemis-dependent.

Catalytic subunit of DNA-dependent protein kinase (DNA-PKcs) is required for HU-induced DSB formation. Since the inhibition of DNA-PKcs kinase activity affects the endonuclease activity of Artemis,[6] we investigated whether suppression of DNA-PKcs kinase activity by the specific inhibitor NU7026 affects DSB formation and subsequent ATM activation. Indeed, NU7026 attenuated DSB formation measured by PFGE (Fig. 6a,b) and neutral comet assay (Fig. S7a,b). Identical results were obtained with the DNA-PKcs-deficient human glioma cell line M059J and parental control M059K by neutral comet assay (Fig. S7c,d). NU7026 attenuated subsequent activation of ATM signaling after 24 h HU exposure (Fig. 6c). Taken together, these results suggest that DNA-PKcs is initially autophosphorylated in response to single-stranded gap DNA lesions at stalled replication forks, which leads to DSB induction mediated by Artemis nuclease and subsequent activation of the ATM signaling pathway.

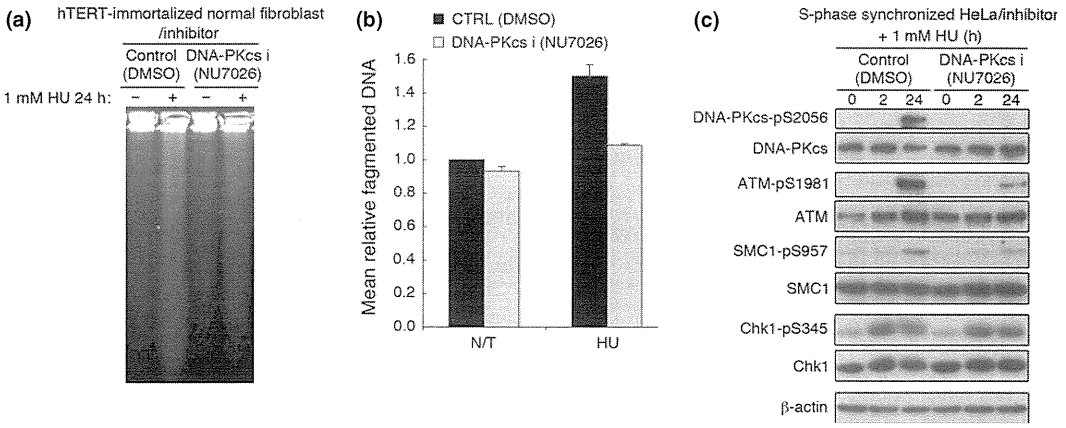

Fig. 6. Double-strand breaks (DSB) generation and ataxia–telangiectasia mutatedactivation (ATM) activation following prolonged replication fork stalling are dependent on catalytic subunit of DNA-dependent protein kinase (DNA-PKcs) activity. (a) Normal human fibroblasts (HDF2/326) were pretreated with DMSO or 10 μM NU7026 for 1 h, and treated with 1 mM HU for 24 h in the presence or absence (DMSO) of NU7026 (10 μM). Cells were analyzed by pulse field gel electrophoresis (PFGE). (b) Mean relative fragmented DNA (1 = the average of the fraction of DNA released from the gel plug in untreated control) from (a) was calculated, and data are shown in the bar graph. Data represent the mean ± SEM from two independent experiments. (c) S-phase synchronized HeLa cells were treated with 1 mM HU 1 h after release from double thymidine block with DMSO or NU7026 (10 μM). Cell extracts from the indicated time points were immunoblottedwith the indicated antibodies.

Discussion

We revealed that the Artemis/DNA-PK machinery plays a critical role in generating DSBs after prolonged replication fork stalling by continuous HU exposure. Involvement of some nucleases has been speculated. Recently, the endonuclease Mus81 was shown to be involved in DSB formation after prolonged inhibition of DNA replication by HU and aphidicolin in mouse embryonic stem cells.[19] Mus81 was also shown to interact with human Apollo/SNM1B, a member of the SNM1 nuclease family characterized by the presence of a metallo-β-lactamase domain, and they have been speculated to work cooperatively for DSB formation after replication stress.[29] Because Artemis/SNM1C is also a member of the SNM1 nuclease family, we hypothesized that, like Apollo/SNM1B, Artemis/SMN1C also works cooperatively with Mus81. However, Artemis and Mus81 did not associate with each other before or after HU exposure (data not shown), suggesting that these proteins might function independently against different targets/substrates. For example, Artemis can cleave hairpin or bubble structures, but Mus81 does not process these structures.[30]

After replication fork stalling, secondary structures such as hairpins, stem-loops/bubbles, or similar structures might be formed on ssDNA gaps.[31,32] There is a strong possibility that these secondary structures activate DNA-PK, and are processed by Artemis on the stalled replication fork *in cellulo*. This is in accord with the idea that autophosphorylation and simultaneous conformational changes in DNA-PK enhance cleavage of ssDNA–dsDNA junctions by Artemis.[6,33]

Replication-associated DSBs are thought to be one-sided DSBs, and can cause chromosomal aberrations such as translocation, when these one-sided DSBs are rejoined with incorrect partners. Indeed, replication-associated DSBs are thought to be tumorigenic.[34,35] Thus, genome integrity during replication needs to be monitored by several fail-safe mechanisms. Increase of DSB generation and apoptosis induction is one of the ways to avoid tumorigenesis in Artemis-competent cells. In contrast, induction of apoptosis was impaired and cellular survival was increased with fewer DSBs in Artemis-deficient fibroblasts after prolonged

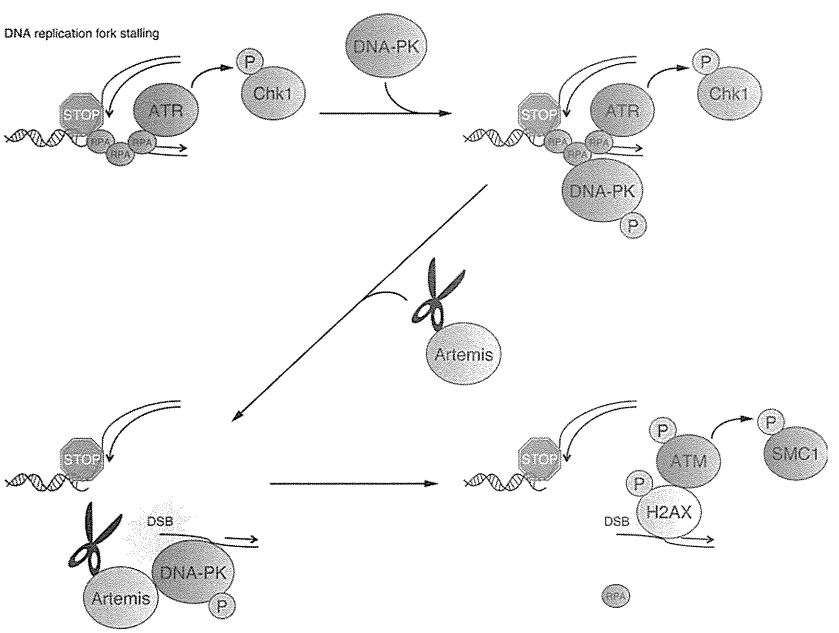

Fig. 7. Model for Artemis-mediated double-strand break (DSB) formation and subsequent DNA damage checkpoint activation. ATM, ataxia–telangiectasia mutated; ATR, ataxia–telangiectasia and RAD3-related; DNA-PK, DNA-dependent protein kinase; P, phosphorylation; RPA, replication protein A.

doi: 10.1111/cas.12144

HU.[36] Artemis-deficient fibroblasts may have aberrant chromosomes in M-phase after prolonged HU treatment, as is the case in Mus81-knockout embryonic stem cells,[19] but fail to be eradicated by cell death through apoptosis/mitotic catastrophe. These are in accord with the recent finding that apoptosis induction after massive DSB is Artemis-dependent.[37] Thus, further study is ongoing in order to assess whether genomic abnormalities increase in Artemis-deficient fibroblasts surviving after HU-induced replication stress.

In summary, our findings indicate a novel function of the DNA nuclease Artemis in resolving stalled DNA replication forks in cells in S phase, with potential implications for understanding carcinogenesis and therapeutic responses to DNA damaging drugs. Although stalled replication forks initially activate an ATR-dependent DNA damage response, when stalling is prolonged, cells may trigger a second wave of DNA damage checkpoint response mediated by Artemis-dependent DSB generation (Fig. 7). Thus, Artemis plays an essential role in the response to DNA damage caused by HU-induced replication fork stalling. Subsequent activation of the ATM signaling pathway in response to DSB generation could allow two alternative cell fates through either induction of cell death or DSB-dependent DNA repair/replication restart, thereby preventing the disruption of DNA integrity.

Acknowledgments

We thank Dr. Leonard Wu (University of Oxford, Oxford, UK) for providing the pG68 and pG48 plasmids, and Dr. Minoru Takata (Kyoto University, Kyoto, Japan) for providing the Artemis expression plasmid. We also thank N. Terada and M. Sato for characterizing Artemis-deficient fibroblasts by genomic PCR, S. Nakada, A. Shibata, R. Sakasai, and Y. Ichijima for inspiring discussions, and the members of the H.T. and S.M. laboratories for helpful discussions. This work was supported by a Grant-in-Aid from the Ministry of Education, Science, and Culture (Japan) to S.M. and by a Grant-in-Aid for Cancer Research from the Ministry of Health, Labor and Welfare (Japan) to S.M. and M.T.

Disclosure Statement

The authors have no conflicts of interest.

Abbreviations

ATM	ataxia–telangiectasia mutated
ATR	ataxia–telangiectasia and RAD3-related
DNA-PK	DNA-dependent protein kinase
DNA-PKcs	catalytic subunit of DNA-dependent protein kinase
dsDNA	double-stranded DNA
DSB	double-strand break
γH2AX	phosphorylated histone H2AX
hTERT	human telomerase reverse transcriptase
HU	hydroxyurea
PFGE	pulse field gel electrophoresis
RPA	replication protein A
RS-SCID	radiosensitive severe combined immunodeficiency
shRNA	short hairpin RNA
siATR	short interfering RNA against ATR
siRNA	short interfering RNA
ssDNA	single-stranded DNA

References

1 Cimprich KA, Cortez D. ATR: an essential regulator of genome integrity. *Nat Rev Mol Cell Biol* 2008; **9**: 616–27.
2 Falck J, Coates J, Jackson SP. Conserved modes of recruitment of ATM, ATR and DNA-PKcs to sites of DNA damage. *Nature* 2005; **434**: 605–11.
3 Bakkenist CJ, Kastan MB. DNA damage activates ATM through intermolecular autophosphorylation and dimer dissociation. *Nature* 2003; **421**: 499–506.
4 Jazayeri A, Falck J, Lukas C, *et al.* ATM- and cell cycle-dependent regulation of ATR in response to DNA double-strand breaks. *Nat Cell Biol* 2006; **8**: 37–45.
5 Branzei D, Foiani M. Regulation of DNA repair throughout the cell cycle. *Nat Rev Mol Cell Biol* 2008; **9**: 297–308.
6 Goodarzi AA, Yu Y, Riballo E, *et al.* DNA-PK autophosphorylation facilitates Artemis endonuclease activity. *EMBO J* 2006; **25**: 3880–9.
7 Ma Y, Schwarz K, Lieber MR. The Artemis: DNA-PKcs endonuclease cleaves DNA loops, flaps, and gaps. *DNA Repair (Amst)* 2005; **4**: 845–51.
8 Riballo E, Kuhne M, Rief N, *et al.* A pathway of double-strand break rejoining dependent upon ATM, Artemis, and proteins locating to gamma-H2AX foci. *Mol Cell* 2004; **16**: 715–24.
9 Kobayashi N, Agematsu K, Sugita K, *et al.* Novel Artemis gene mutations of radiosensitive severe combined immunodeficiency in Japanese families. *Hum Genet* 2003; **112**: 348–52.
10 Stiff T, Walker SA, Cerosaletti K, *et al.* ATR-dependent phosphorylation and activation of ATM in response to UV treatment or replication fork stalling. *EMBO J* 2006; **25**: 5775–82.
11 Sakasai R, Shinohe K, Ichijima Y, *et al.* Differential involvement of phosphatidylinositol 3-kinase-related protein kinases in hyperphosphorylation of replication protein A2 in response to replication-mediated DNA double-strand breaks. *Genes Cells* 2006; **11**: 237–46.
12 Brown EJ, Baltimore D. ATR disruption leads to chromosomal fragmentation and early embryonic lethality. *Genes Dev* 2000; **14**: 397–402.
13 Zhao H, Piwnica-Worms H. ATR-mediated checkpoint pathways regulate phosphorylation and activation of human Chk1. *Mol Cell Biol* 2001; **21**: 4129–39.
14 Liu S, Bekker-Jensen S, Mailand N, Lukas C, Bartek J, Lukas J. Claspin operates downstream of TopBP1 to direct ATR signaling towards Chk1 activation. *Mol Cell Biol* 2006; **26**: 6056–64.
15 Matsuoka S, Rotman G, Ogawa A, Shiloh Y, Tamai K, Elledge SJ. Ataxia telangiectasia-mutated phosphorylates Chk2 in vivo and in vitro. *Proc Natl Acad Sci USA* 2000; **97**: 10389–94.
16 Takahashi A, Ohnishi T. Does gammaH2AX foci formation depend on the presence of DNA double strand breaks? *Cancer Lett* 2005; **229**: 171–9.
17 Ward IM, Chen J. Histone H2AX is phosphorylated in an ATR-dependent manner in response to replicational stress. *J Biol Chem* 2001; **276**: 47759–62.
18 Robison JG, Lu L, Dixon K, Bissler JJ. DNA lesion-specific co-localization of the Mre11/Rad50/Nbs1 (MRN) complex and replication protein A (RPA) to repair foci. *J Biol Chem* 2005; **280**: 12927–34.
19 Hanada K, Budzowska M, Davies SL, *et al.* The structure-specific endonuclease Mus81 contributes to replication restart by generating double-strand DNA breaks. *Nat Struct Mol Biol* 2007; **14**: 1096–104.
20 Furuta T, Takemura H, Liao ZY, *et al.* Phosphorylation of histone H2AX and activation of Mre11, Rad50, and Nbs1 in response to replication-dependent DNA double-strand breaks induced by mammalian DNA topoisomerase I cleavage complexes. *J Biol Chem* 2003; **278**: 20303–12.
21 Shi W, Feng Z, Zhang J, *et al.* The role of RPA2 phosphorylation in homologous recombination in response to replication arrest. *Carcinogenesis* 2010; **31**: 994–1002.
22 Chan DW, Chen BP, Prithivirajsingh S, *et al.* Autophosphorylation of the DNA-dependent protein kinase catalytic subunit is required for rejoining of DNA double-strand breaks. *Genes Dev* 2002; **16**: 2333–8.
23 Chen BP, Chan DW, Kobayashi J, *et al.* Cell cycle dependence of DNA-dependent protein kinase phosphorylation in response to DNA double strand breaks. *J Biol Chem* 2005; **280**: 14709–15.
24 Hammarsten O, Chu G. DNA-dependent protein kinase: DNA binding and activation in the absence of Ku. *Proc Natl Acad Sci USA* 1998; **95**: 525–30.
25 Martensson S, Hammarsten O. DNA-dependent protein kinase catalytic subunit. Structural requirements for kinase activation by DNA ends. *J Biol Chem* 2002; **277**: 3020–9.
26 Morozov VE, Falzon M, Anderson CW, Kuff EL. DNA-dependent protein kinase is activated by nicks and larger single-stranded gaps. *J Biol Chem* 1994; **269**: 16684–8.
27 Falzon M, Fewell JW, Kuff EL. EBP-80, a transcription factor closely resembling the human autoantigen Ku, recognizes single- to double-strand transitions in DNA. *J Biol Chem* 1993; **268**: 10546–52.
28 Ralf C, Hickson ID, Wu L. The Bloom's syndrome helicase can promote the regression of a model replication fork. *J Biol Chem* 2006; **281**: 22839–46.

29 Bae JB, Mukhopadhyay SS, Liu L, *et al.* Snm1B/Apollo mediates replication fork collapse and S Phase checkpoint activation in response to DNA interstrand cross-links. *Oncogene* 2008; **27**: 5045–56.
30 Ciccia A, McDonald N, West SC. Structural and functional relationships of the XPF/MUS81 family of proteins. *Annu Rev Biochem* 2008; **77**: 259–87.
31 Burrow AA, Marullo A, Holder LR, Wang YH. Secondary structure formation and DNA instability at fragile site FRA16B. *Nucleic Acids Res* 2010; **38**: 2865–77.
32 Voineagu I, Narayanan V, Lobachev KS, Mirkin SM. Replication stalling at unstable inverted repeats: interplay between DNA hairpins and fork stabilizing proteins. *Proc Natl Acad Sci USA* 2008; **105**: 9936–41.
33 Ding Q, Reddy YV, Wang W, *et al.* Autophosphorylation of the catalytic subunit of the DNA-dependent protein kinase is required for efficient end processing during DNA double-strand break repair. *Mol Cell Biol* 2003; **23**: 5836–48.
34 Bartkova J, Horejsi Z, Koed K, *et al.* DNA damage response as a candidate anti-cancer barrier in early human tumorigenesis. *Nature* 2005; **434**: 864–70.
35 Gorgoulis VG, Vassiliou LV, Karakaidos P, *et al.* Activation of the DNA damage checkpoint and genomic instability in human precancerous lesions. *Nature* 2005; **434**: 907–13.
36 Unno J. Artemis-dependent cell death by prolonged replication fork stalling. *Jpn J Pediatr Hematol.* 2011; **25**: 86–90.
37 Abe T, Ishiai M, Hosono Y, *et al.* KU70/80, DNA-PKcs, and Artemis are essential for the rapid induction of apoptosis after massive DSB formation. *Cell Signal* 2008; **20**: 1978–85.

Supporting Information

Additional Supporting Information may be found in the online version of this article:

Doc. S1. Supplementary experimental procedure.

Fig. S1. Cell cycle distribution of S-phase synchronized HeLa cells, quantification of Figure 1(b); ATM activation in HeLa cells transfected with siATR, quantification of Fig. 1(b) .

Fig. S2. Magnified image of γH2AX and RPA2 foci and signal intensity chromatographs.

Fig. S3. RPA2 and phosphorylated ATM colocalization after hydroxyurea treatment, analyzed by immunofluorescence.

Fig. S4. Camptothecin (CPT) induces double-strand breaks.

Fig. S5. Cell cycle profiles of shRNA transfected HeLa cells.

Fig. S6. Quantitation of immunofluorescence data shown in Figure 5(b). Magnified image of phospho-DNA-PKcs (T2609) and RPA2 fociand signal intensity chromatographs. Artemis-independent activation of DNA-PKcs analyzed by Western blotting and immunofluorescence.

Fig. S7. Generation of DSBs dependent on DNA-PKcs analyzed by comet assay.

doi: 10.1111/cas.12144

J Clin Immunol (2013) 33:857–864
DOI 10.1007/s10875-012-9859-9

ORIGINAL RESEARCH

Rapid Detection of Intracellular p47phox and p67phox by Flow Cytometry; Useful Screening Tests for Chronic Granulomatous Disease

Taizo Wada · Masahiro Muraoka · Tomoko Toma · Tsuyoshi Imai · Tomonari Shigemura · Kazunaga Agematsu · Kohei Haraguchi · Hiroyuki Moriuchi · Tsutomu Oh-ishi · Toshiyuki Kitoh · Osamu Ohara · Tomohiro Morio · Akihiro Yachie

Received: 25 September 2012 / Accepted: 20 December 2012 / Published online: 10 January 2013

Abstract Chronic granulomatous disease (CGD) is caused by defects of NADPH oxidase. The diagnosis of CGD can be made by analysis of NADPH oxidase activity, however, identification of the CGD subgroups is required before performing mutation analysis. The membrane-bound subunits, gp91phox and p22phox, can be quickly analyzed by flow cytometry, unlike the cytosolic components, p47phox and p67phox. We evaluated the feasibility of flow cytometric detection of p47phox and p67phox with specific monoclonal antibodies in two patients with p47phox deficiency and 7 patients with p67phox deficiency. Consistent with previous observations, p47phox and p67phox were expressed in phagocytes and B cells, but not in T or natural killer cells, from normal controls. In contrast, patients with p47phox and p67phox deficiency showed markedly reduced levels of p47phox and p67phox, respectively. These techniques will be useful to rapidly assess the expression of the cytosolic components, p47phox and p67phox, and represents important secondary screening tests for CGD.

Keywords Chronic granulomatous disease · p47phox · p67phox · flow cytometry · screening test

T. Wada (✉) · M. Muraoka · T. Toma · A. Yachie
Department of Pediatrics, School of Medicine, Institute of Medical, Pharmaceutical and Health Sciences, Kanazawa University, 13-1 Takaramachi,
Kanazawa 920-8641, Japan
e-mail: taizo@staff.kanazawa-u.ac.jp

T. Imai
Department of Pediatrics, Otsu Red-Cross Hospital, Otsu, Japan

T. Shigemura · K. Agematsu
Department of Pediatrics, Shinshu University School of Medicine, Matsumoto, Japan

K. Haraguchi · H. Moriuchi
Department of Pediatrics, Nagasaki University Hospital, Nagasaki, Japan

T. Oh-ishi
Division of Infectious Diseases, Immunology, and Allergy, Saitama Children's Medical Center, Saitama, Japan

T. Kitoh
Department of Pediatrics, Aichi Medical University, Nagakute, Japan

O. Ohara
Kazusa DNA research Institution, Chiba, Japan

T. Morio
Department of Pediatrics, Tokyo Medical and Dental University, Tokyo, Japan

Introduction

Chronic granulomatous disease (CGD) is a primary immunodeficiency disease of phagocytes caused by defects of nicotinamide dinucleotide phosphate (NADPH) oxidase [1, 2]. NADPH oxidase is an enzyme responsible for the production of reactive oxygen species that are needed to kill pathogenic bacteria and fungi. Patients with CGD have increased susceptibility to infections, as well as hyperinflammation and granuloma formation at sites of infection [3]. The NADPH oxidase is a multicomponent system including a membrane-bound flavocytochrome b558, comprised of gp91phox and p22phox, cytosolic components,

comprised of p40phox, p47phox, and p67phox, and a small GTP-binding protein comprised of Rac1 or Rac2 [1, 2]. About 70 % of CGD cases are caused by mutations in the *CYBB* gene that encodes gp91phox and is located at Xp21.1 [4]. The remaining 30 % of cases include four other subgroups of the disease, all of which are inherited in an autosomal recessive manner [1, 2]. Mutations in the *NCF1* gene cause p47phox deficiency, the second most common subtype of CGD, which accounts for 25 % of CGD patients. The other cases occur due to mutations in the *NCF2*, *CYBA*, or *NCF4* genes that encode p67phox, p22phox, or p40phox, respectively. To date, p40phox deficiency has only been reported in one individual [5].

A diagnosis of CGD can be achieved by measurement of neutrophil superoxide production via NADPH oxidase. The most recognized test is the nitroblue tetrazolium test, which is based on visual inspection of phagocytes. Because of its high reliability and sensitivity, the dihydrorhodamine (DHR) assay using flow cytometry has largely replaced the nitroblue tetrazolium test in many laboratories [6]. Despite the need for specific technical skills, the DHR assay is able to distinguish between patients with absent to greatly diminished production of superoxide, which is commonly observed in males with X-linked CGD and patients with residual superoxide production, which is frequently observed in autosomal recessive and variant X-linked CGD [1, 2]. However, further identification of CGD subgroups is necessary before genetic analysis, which is often labor-intensive and time-consuming. The membrane-bound subunits, gp91phox and p22phox, can be analyzed by flow cytometry using monoclonal antibodies (mAbs), such as 7D5 that identifies the extracellular domain of flavocytochrome b558 [7, 8]. In contrast, the cytosolic components, p47phox and p67phox, are usually investigated by immunoblot analysis that requires a large sample of blood and takes longer to perform. We therefore assessed the feasibility of flow cytometric analysis of intracellular p47phox and p67phox expression and demonstrate its usefulness as a secondary screening test for CGD.

Materials and Methods

Patients

We studied nine affected patients with autosomal recessive CGD: two with p47phox deficiency and seven with p67phox deficiency. All patients but p67-4 were born to non-consanguineous Japanese parents. We also evaluated three patients with X-linked CGD (gp91phox deficiency) and ten healthy adult volunteers. Case presentations of patients p47-1 and p47-2 and the sibling cases of p67-1.1 and p67-1.2 have been reported elsewhere [9, 10]. Patients p67-2.1 and p67-2.2 were also sibling cases. Approval for the study was obtained from the Human Research Committee of Kanazawa University Graduate School of Medical Science, and informed consent was obtained in accordance with the Declaration of Helsinki.

Flow Cytometry

For the analysis of p47phox and p67phox expression, peripheral blood mononuclear cells (PBMCs) were isolated by Ficoll-Hypaque gradient centrifugation from patients and controls immediately after blood collection or after overnight shipment at ambient temperature. Granulocytes were recovered from the pellet of the gradient after lysis of any erythrocytes. PBMCs were stained for cell-surface antigens before cell membrane permeabilization using the following mAbs: fluorescein isothiocyanate-conjugated anti-CD14 and anti-CD56; phycoerythrin-Cy5-conjugated anti-CD20 and anti-CD3 (all from Becton Dickinson, San Diego, CA). Granulocytes were stained with fluorescein isothiocyanate-conjugated anti-CD16b mAb (Beckman Coulter, Fullerton, CA). After washing, cells were fixed and permeabilized with Cytofix/Cytoperm Plus kit (Becton Dickinson) and were incubated with anti-p47phox (clone 1, Becton Dickinson), anti-p67phox mAb (clone D-6, Santa Cruz Biotechnology Inc, Santa Cruz, CA) or purified mouse IgG1 (Becton Dickinson) at 4 °C for 20 min. Cells were then reacted with phycoerythrin-conjugated anti-mouse IgG1 (Southern Biotech, Birmingham, AL) at 4 °C for 20 min. Stained cells were analyzed with a FACSCalibur flow cytometer using CellQuest software (BD Bioscience, Tokyo, Japan) [11]. Because the anti-p47phox and anti-p67phox mAbs belong to the mouse IgG1 subclass, all antibodies for surface staining were chosen from mouse IgG2 or IgM to avoid cross-reaction. For analysis of gp91phox and p22phox, whole blood was stained with 7D5 mAb (MBL, Nagoya, Japan).

Analysis of the Production of Reactive Oxygen Species

Peripheral blood was loaded with 1 μM of DHR 123 at 37°C for 5 min, and stimulated with 100 ng/mL of phorbol myristate acetate at 37°C for 30 min. After lysis of erythrocytes, production of reactive oxygen species of granulocytes was quantified by measuring intracellular rhodamine using flow cytometry, as previously described [9, 12].

Mutation Analysis of NCF1 and NCF2

DNA was extracted from blood samples using standard methods. The *NCF1* and *NCF2* genes were amplified from specific primers as previously described [9]. Sequencing was performed on purified polymerase chain reaction products using the ABI Prism BigDye Terminator Cycle sequencing kit on an

ABI 310 or 3100 automated sequencer (Applied Biosystems, Foster, CA) [13].

Results

Mutation Analysis and Production of Reactive Oxygen Species

Table I presents the clinical and sequencing data of the patients. Patients p67-2.1 and p67-2.2 were compound heterozygotes bearing Gln260X and Arg395Trp mutations in *NCF2*. The former is a novel nonsense mutation. Two distinct *NCF2* mutations, Tyr394Asp and Asp408fs, were demonstrated in patient p67-3. The effect of the novel missense mutation Tyr394Asp was evaluated using the web-based analysis tool, Mutation@A Glance (http://rapid.rcai.riken.jp/mutation/) [14], and was found to be deleterious on the basis of the SIFT program [15]. Patient P67-5 was a compound heterozygote bearing Trp22X and Arg102X mutations. The former is a novel nonsense mutation.

Upon stimulation with phorbol myristate acetate, DHR-loaded neutrophils from normal controls showed significant increases in fluorescence with tight peaks. Patients with gp91phox deficiency exhibited virtually no neutrophil DHR activity. In contrast, patients with p47phox or p67phox deficiency exhibited variable activity ranging from almost none to a moderate increase in the fluorescence after stimulation with characteristic wider peaks compared with those found in gp91phox deficiency.

Intracellular Expression of p47phox and p67phox

Consistent with previous observations [2], p47phox and p67phox were expressed intracellularly in phagocytes and B cells, but not in T or natural killer (NK) cells, from normal controls (Fig. 1). This pattern of lineage-specific expression was the same as that observed for gp91phox expression. However, we observed a marked difference in p47phox or p67phox expression among neutrophils, monocytes and B cells, which was in contrast to the expression of gp91phox. The p47phox levels in neutrophils were relatively low compared with monocytes and B cells, whereas the p67phox levels in B cells were considerably lower compared with neutrophils and monocytes. Because neutrophils exhibited decreased viability and tended to aggregate after overnight shipment and cell isolation, we decided to use PBMCs for intracellular staining of p47phox and p67phox in clinical samples in order to avoid non-specific staining that might lead to misdiagnosis.

The patients with p47phox deficiency exhibited markedly reduced levels of p47phox expression in both monocytes and B cells (Fig. 2). Conversely, the patients' monocytes and B cells expressed p67phox at levels that were comparable to normal controls. On the other hand, the patients with p67phox deficiency exhibited considerably reduced levels of p67phox expression in monocytes and B cells (Fig. 2). Although the expression of p47phox in the monocytes appeared to be marginally decreased, p47phox expression in the patients' B cells was comparable to normal controls. Expression of the membrane-bound component, gp91phox, determined by 7D5 mAb, was normal in all patients with p47phox and p67phox deficiency.

Expression of p47phox or p67phox in Carrier Parents

To evaluate the ability of our flow cytometric analysis technique to detect carriers, we examined p47phox expression in monocytes from the parents of p47-1 and p67phox expression in monocytes from the mother of p67-2.1 and p67-2.2 and the parents of p67-3, all of whom were heterozygous carriers (Fig. 3). The pattern of DHR and gp91phox

Table I Clinical and sequencing data

Subjects	Age[a]	Clinical features	Gene	Nucleotide mutation	Effect
p47-1	31 years	Skin infections, otitis, colitis	*NCF1*	73_74delGT[d]	Tyr26fs
p47-2	13 years	BCGitis Williams syndrome	*NCF1*	73_74delGT 7q11.23 deletion	Tyr26fs
p67-1.1[b]	8 years	Perianal abscess, lymphadenitis	*NCF2*	1223delA[d]	Asp408fs
p67-1.2[b]	2 years	Perianal abscess	*NCF2*	1223delA[d]	Asp408fs
p67-2.1[c]	1 month	Aspergillus pneumonia	*NCF2*	778C>T 1183C>T	Gln260X Arg395Trp
p67-2.2[c]	3 years	Sepsis	*NCF2*	778C>T 1183C>T	Gln260X Arg395Trp
p67-3	6 month	Aspergillus pneumonia	*NCF2*	1180T>G 1223delA	Tyr394Asp Asp408fs
p67-4	10 month	BCGitis	*NCF2*	304C>T[d]	Arg102X
p67-5	5 years	BCGitis lymphadenitis	*NCF2*	66G>A 304C>T	Trp22X Arg102X

[a] Data at the time of sample collection

[b,c] Sibling cases

[d] Homozygous mutation

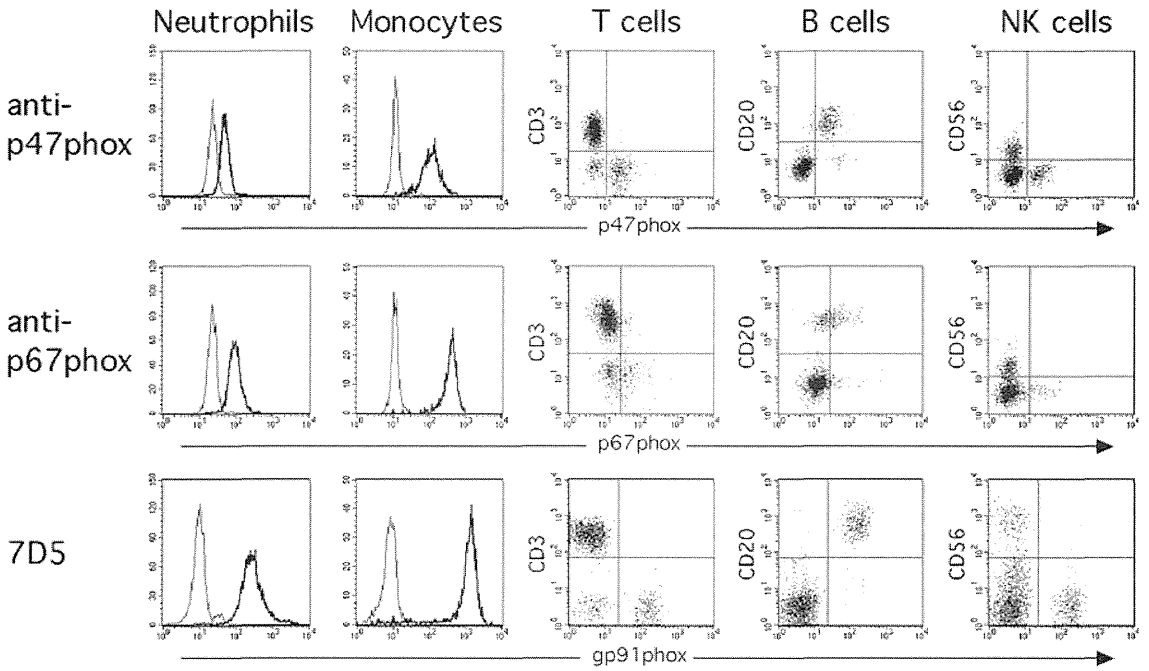

Fig. 1 Expression of p47phox, p67phox and gp91phox in blood leukocyte populations from normal individuals. Shown are the results of intracellular expression of p47phox (*top*) and p67phox (*middle*), and surface expression of gp91phox analyzed by 7D5mAb (*bottom*) in $CD16b^+$ neutrophils, $CD14^+$ monocytes, $CD3^+$ T, $CD20^+$ B, and $CD56^+$ NK cells from a healthy control. Thin lines indicate control Ab; thick lines represent mAbs specific for the NADPH subunits

expression from the mother of gp91-1 showed a bimodal distribution consistent with her obligate X-linked CGD carrier status. In contrast, and consistent with previous reports [2], the NADPH oxidase activities of neutrophils from carriers of the p47phox and p67phox deficiency were normal. The expression of p47phox or p67phox in their monocytes appeared to be decreased slightly, compared with normal controls (Fig. 3).

Discussion

In the present study, we have developed practical flow cytometric assays for p47phox and p67phox. Although analysis of the expression of the individual subunits by flow cytometry has been described previously [16], our approach differs from it on two counts. First, we used commercially available mAbs that are specific for p47phox and p67phox. This potential advantage may allow the assay to be widely used in many laboratories. Second, we analyzed the intracellular expression of p47phox and p67phox in monocytes and B cells, as well as in neutrophils. B cells contain all of the components of the phagocyte NADPH oxidase and generate superoxide in response to a variety of stimuli; albeit at a lower level than neutrophils [17]. Our lineage-specific analysis may provide more accurate and reliable data. Previous studies using Western blot analysis have demonstrated that p47phox and p67phox expression in B cells were reduced by about 6 and 70 %, respectively, compared with neutrophils [17]. The reasons neutrophils from normal individuals exhibited lower levels of p47phox compared with monocytes and B cells in our assay are presently unclear. Further studies using other anti-p47phox antibodies that recognize different epitopes will be necessary to resolve this issue.

The NADPH subunits including p47phox, p67phox and p40phox exist as a tight complex in the cytoplasm in the resting state [18]. However, loss of one of the p47phox or p67phox proteins did not generally affect the expression of the other, unlike the membrane-bound components, gp91phox and p22phox. Because gp91phox and p22phox act to stabilize each other, and the absence of either protein generally leads to down-regulation of the other [19, 20]. In fact, the 7D5mAb that binds exclusively to an extracellular domain of gp91phox has been proven not to stain the cell surface on neutrophils deficient in p22phox, thus indicating its screening capability for both gp91phox and p22phox deficiency [8]. Therefore, the combined flow cytometric analysis of the surface staining by 7D5mAb and our assay for intracellular p47phox and p67phox would be a valuable tool for detecting subgroups of CGD.

Mutations in the gp91phox gene cause X-linked CGD and account for approximately 70 % of all cases [4]. The remaining 30 % are due to mutations in the other subunit and are inherited in an autosomal recessive manner [1]. In Japan, p47phox-deficient CGD has been documented in relatively few patients, unlike Western countries [21].

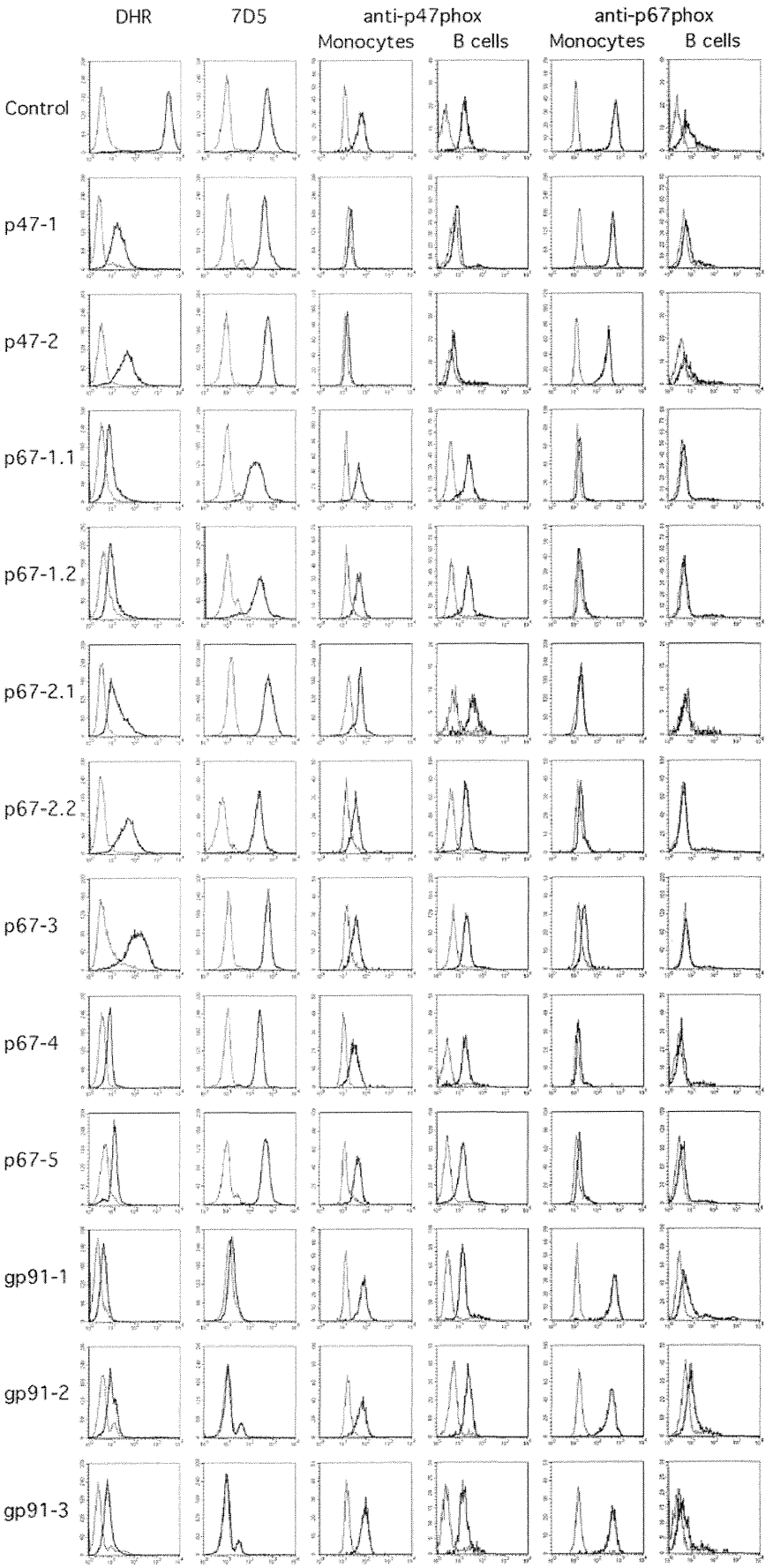

Fig. 2 Analysis of DHR and expression of p47phox, p67phox and gp91phox in CGD patients. In the DHR assay, granulocytes were analyzed using DHR 123 as a fluorescent probe before (*thin lines*) and after (*thick lines*) stimulation with phorbol myristate acetate. Expression of gp91phox in granulocytes, as assessed using 7D5, and expression of p47phox and p67phox in $CD14^+$ monocytes and $CD20^+$ B cells are shown

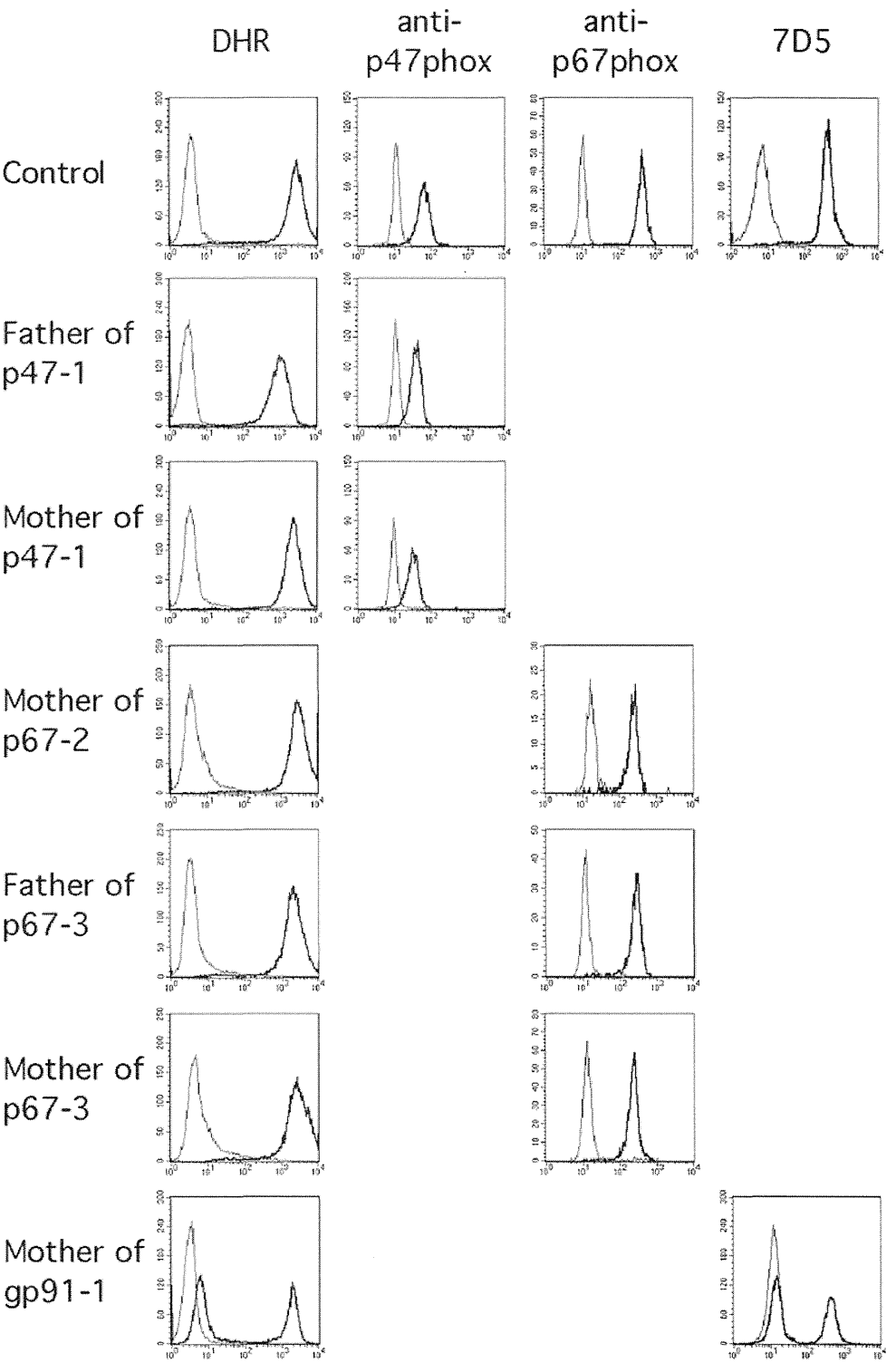

Fig. 3 DHR assay and expression of p47phox or p67phox in carrier parents. Rhodamine expression in unstimulated and phorbol myristate acetate-stimulated granulocytes obtained from obligate carriers. Expression of gp91phox analyzed using 7D5 in granulocytes and the expression of p47phox or p67phox in $CD14^+$ monocytes are shown

Because of the infrequency of such diseases, our study was limited to include a small number of patients, in particular, those with p47phox deficiency. However, the vast majority of patients with p47phox deficiency carry the homozygous 2-bp deletion in the *NCF1* gene, which was also detected in our patients. This mutation results from recombination events between the wild-type gene and the pseudogene [22, 23]. Patients with this mutation have been reported to exhibit undetectable levels of p47phox protein expression [23], which was consistent with our results. On the other hand, although a variety of mutations in the *NCF2* gene have been demonstrated in patients with p67phox deficiency, the p67phox protein appears to be undetectable by Western blot analysis in most cases [23]. Interestingly, the

p67phox protein was absent in patients p67-1.1, p67-1.2, p67-2.1, p67-2.2, p67-4 and p67-5, whereas residual p67phox expression was detected in patient p67-3 who exhibited the significant remaining NADPH oxidase activity. It should be noted that there are mutations in the *NCF1* or *NCF2* genes that leave the protein expression intact but destroy the enzymatic activity [23]. In such cases, albeit rare, our flow cytometric analysis of protein expression as well as Western blot analysis cannot contribute to identification of the CGD subgroups, and mutation analysis is required. Further investigations will be required to assess the sensitivity and limitations of the assay and its utility in determining the phenotype-genotype correlation.

Most female carriers of X-linked CGD can be identified by flow cytometry. A mosaic pattern of oxidase-positive and -negative neutrophils from the basis of the DHR assay or analysis of gp91phox expression is observed due to random X-chromosome inactivation. In contrast, the detection of carriers of autosomal recessive CGD is usually performed by genetic analysis. It is well known that the NADPH oxidase activity is normal in obligate carriers [2]. The expression of p47phox and p67phox proteins, assessed by Western blot analysis, has also been reported to likely be normal in carriers of p47phox and p67phox deficiency, respectively [2]. Our flow cytometric analysis demonstrated slightly decreased expression of p47phox and p67phox in monocytes from obligate carriers of p47phox and p67phox deficiency, respectively, compared with normal controls. However, these subtle differences of protein expression do not allow the detection of carriers in the clinical settings. Therefore, genetic testing remains appropriate for identification of carriers of autosomal recessive CGD.

In summary, our study demonstrated rapid and sensitive detection of intracellular p47phox and p67phox by flow cytometry, which is useful as a secondary screening test for CGD. This technique would be also valuable in the evaluation of chimerism in patients treated with stem cell transplantation or gene therapy.

Acknowledgments We thank Dr. Fabio Candotti for insightful discussions, and Ms Harumi Matsukawa, Ms. Shizu Kouraba and Ms. Miho Nishio for their excellent technical assistance. This work was supported by a grant from Morinaga Houshikai, Tokyo; a Grant-in-Aid for Scientific Research from the Ministry of Education, Culture, Sports, Science and Technology of Japan; and a grant from the Ministry of Health, Labour, and Welfare of Japan, Tokyo.

Conflict of Interest The authors declare that they have no conflict of interest.

References

1. Holland SM. Chronic granulomatous disease. Clin Rev Allergy Immunol. 2010;38(1):3–10. doi:10.1007/s12016-009-8136-z.
2. Roos D, Kuijpers TW, Curnutte JT. Chronic granulomatous disease. Second ed. Primary immunodeficiency diseases. New York: Oxford Universtiy Press; 2007.
3. Rosenzweig SD. Inflammatory manifestations in chronic granulomatous disease (CGD). J Clin Immunol. 2008;28 Suppl 1:S67–72. doi:10.1007/s10875-007-9160-5.
4. Roos D, Kuhns DB, Maddalena A, Roesler J, Lopez JA, Ariga T, et al. Hematologically important mutations: X-linked chronic granulomatous disease (third update). Blood Cells Mol Dis. 2010;45(3):246–65. doi:10.1016/j.bcmd.2010.07.012.
5. Matute JD, Arias AA, Wright NA, Wrobel I, Waterhouse CC, Li XJ, et al. A new genetic subgroup of chronic granulomatous disease with autosomal recessive mutations in p40 phox and selective defects in neutrophil NADPH oxidase activity. Blood. 2009;114(15):3309–15. doi:10.1182/blood-2009-07-231498.
6. Vowells SJ, Fleisher TA, Sekhsaria S, Alling DW, Maguire TE, Malech HL. Genotype-dependent variability in flow cytometric evaluation of reduced nicotinamide adenine dinucleotide phosphate oxidase function in patients with chronic granulomatous disease. J Pediatr. 1996;128(1):104–7.
7. Nakamura M, Murakami M, Koga T, Tanaka Y, Minakami S. Monoclonal antibody 7D5 raised to cytochrome b558 of human neutrophils: immunocytochemical detection of the antigen in peripheral phagocytes of normal subjects, patients with chronic granulomatous disease, and their carrier mothers. Blood. 1987;69(5):1404–8.
8. Burritt JB, DeLeo FR, McDonald CL, Prigge JR, Dinauer MC, Nakamura M, et al. Phage display epitope mapping of human neutrophil flavocytochrome b558. Identification of two juxtaposed extracellular domains. J Biol Chem. 2001;276(3):2053–61. doi:10.1074/jbc.M006236200.
9. Honda F, Hane Y, Toma T, Yachie A, Kim ES, Lee SK, et al. Transducible form of p47phox and p67phox compensate for defective NADPH oxidase activity in neutrophils of patients with chronic granulomatous disease. Biochem Biophys Res Commun. 2012;417(1):162–8. doi:10.1016/j.bbrc.2011.11.077.
10. Kabuki T, Kawai T, Kin Y, Joh K, Ohashi H, Kosho T, et al. A case of Williams syndrome with p47-phox-deficient chronic granulomatous disease. Nihon Rinsho Meneki Gakkai Kaishi. 2003;26(5):299–303.
11. Wada T, Schurman SH, Otsu M, Garabedian EK, Ochs HD, Nelson DL, et al. Somatic mosaicism in Wiskott–Aldrich syndrome suggests in vivo reversion by a DNA slippage mechanism. Proc Natl Acad Sci U S A. 2001;98(15):8697–702. doi:10.1073/pnas.151260498.
12. Kasahara Y, Iwai K, Yachie A, Ohta K, Konno A, Seki H, et al. Involvement of reactive oxygen intermediates in spontaneous and CD95 (Fas/APO-1)-mediated apoptosis of neutrophils. Blood. 1997;89(5):1748–53.
13. Asai E, Wada T, Sakakibara Y, Toga A, Toma T, Shimizu T, et al. Analysis of mutations and recombination activity in RAG-deficient patients. Clin Immunol. 2011;138(2):172–7. doi:10.1016/j.clim.2010.11.005.
14. Hijikata A, Raju R, Keerthikumar S, Ramabadran S, Balakrishnan L, Ramadoss SK, et al. Mutation@A Glance: an integrative web application for analysing mutations from human genetic diseases. DNA Res. 2010;17(3):197–208. doi:10.1093/dnares/dsq010.
15. Ng PC, Henikoff S. SIFT: Predicting amino acid changes that affect protein function. Nucleic Acids Res. 2003;31(13):3812–4.
16. Yu G, Hong DK, Dionis KY, Rae J, Heyworth PG, Curnutte JT, et al. Focus on FOCIS: the continuing diagnostic challenge of autosomal recessive chronic granulomatous disease. Clin Immunol. 2008;128(2):117–26. doi:10.1016/j.clim.2008.05.008.
17. Dusi S, Nadalini KA, Donini M, Zentilin L, Wientjes FB, Roos D, et al. Nicotinamide-adenine dinucleotide phosphate oxidase assembly and activation in EBV-transformed B lymphoblastoid cell

lines of normal and chronic granulomatous disease patients. J Immunol. 1998;161(9):4968–74.
18. Lapouge K, Smith SJ, Groemping Y, Rittinger K. Architecture of the p40-p47-p67phox complex in the resting state of the NADPH oxidase. A central role for p67phox. J Biol Chem. 2002;277 (12):10121–8. doi:10.1074/jbc.M112065200.
19. Parkos CA, Dinauer MC, Jesaitis AJ, Orkin SH, Curnutte JT. Absence of both the 91kD and 22kD subunits of human neutrophil cytochrome b in two genetic forms of chronic granulomatous disease. Blood. 1989;73(6):1416–20.
20. Verhoeven AJ, Bolscher BG, Meerhof LJ, van Zwieten R, Keijer J, Weening RS, et al. Characterization of two monoclonal antibodies against cytochrome b558 of human neutrophils. Blood. 1989;73 (6):1686–94.
21. Ishibashi F, Nunoi H, Endo F, Matsuda I, Kanegasaki S. Statistical and mutational analysis of chronic granulomatous disease in Japan with special reference to gp91-phox and p22-phox deficiency. Hum Genet. 2000;106(5):473–81.
22. Gorlach A, Lee PL, Roesler J, Hopkins PJ, Christensen B, Green ED, et al. A p47-phox pseudogene carries the most common mutation causing p47-phox- deficient chronic granulomatous disease. J Clin Invest. 1997;100(8):1907–18. doi:10.1172/JCI119721.
23. Roos D, Kuhns DB, Maddalena A, Bustamante J, Kannengiesser C, de Boer M, et al. Hematologically important mutations: the autosomal recessive forms of chronic granulomatous disease (second update). Blood Cells Mol Dis. 2010;44(4):291–9. doi:10.1016/j.bcmd.2010.01.009.